Dissertations, Theses, and Masters Projects   Theses, Dissertations, & Master Projects

1986

Peroxo Complexes of Vanadium(V) and Molybdenum(VI) with Nicotine and Aspartic Acids

Sandra Jean Sheffield
College of William & Mary - Arts & Sciences

Follow this and additional works at: https://scholarworks.wm.edu/etd

Part of the Inorganic Chemistry Commons, and the Organic Chemistry Commons

PEROXO COMPLEXES OF VANADIUM(V) AND MOLYBDENUM(VI)

WITH NICOTINIC AND ASPARTIC ACIDS

A Thesis

Presented to

The Faculty of the Department of Chemistry

The College of William and Mary in Virginia

In Partial Fulfillment

Of the Requirements for the Degree of

Master of Arts

---

by

Sandra J. Sheffield
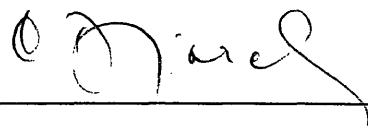

May, 1986

APPROVAL SHEET

This thesis is submitted in partial fulfillment of the

requirements for the degree of

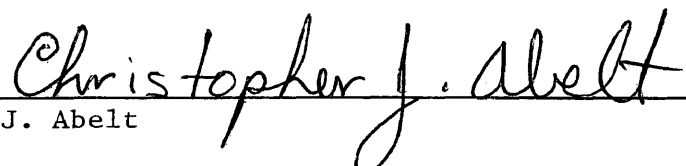Master of Arts

Author /s/ J. Sheffield

Approved, May, 1986

C. Djordjevic

R. C. Coleman

C. J. Abelt

ii

TABLE OF CONTENTS

iii

ACKNOWLEDGEMENTS

LIST OF TABLES

r

LIST OF FIGURES

ABSTRACT

The complex compounds of V(V) and Mo(VI) with peroxo groups and bioligands are of interest in inorganic bio-chemistry. We have investigated the peroxo systems of V(V) and Mo(VI) with nicotinic and aspartic acids. Complexes of the formula $K[VO(O_2)_2NAH]*H_2O$, $[MoO(O_2)_2NAH]*H_2O$, and $M^I[MoO(O_2)_2NA]*H_2O$ where $NAH = C_6H_5NO_2$, and $M = K^+$ or NH_4^+ have been prepared with the nicotinic acid, NAH. Complexes of the formula $K_x[MoO(O_2)_yAsp_z]*H_2O$ and $K_3[VO(O_2)_2Asp_2]$ have been prepared with the aspartic acid, Asp.

These complexes are stable in air and represent the first peroxo-nicotinic acid and peroxo-aspartic acid ligand com-binations, respectively, that have been reported. The IR spectra indicate the presence of a coordinated carboxylato group for each complex and strong bands due to the M=O and coordinated O-O stretchings appear near 950 and 870 cm^{-1}, respectively. Peroxo to metal charge transfer bands in UV-V spectra are found between 400 and 250 nm in both aqueous solution and in the solid state. The complexes are soluble in water, where the cyclic voltamograms show two and three reduction peaks for vanadium and molybdenum, respectively.

PEROXO COMPLEXES OF VANADIUM(V) AND MOLYBDENUM(VI)

WITH NICOTINIC AND ASPARTIC ACIDS

1.0. INTRODUCTION

Molybdenum and vanadium are interesting elements to study. Each displays a variety of oxidation states, coordination numbers, and stereochemistries. Both elements are essential for life and are therefore of interest in biochemistry.

Molybdenum and vanadium peroxo complexes are of interest as catalysts for oxidations and Mo peroxo complexes have been utilized for the oxidation of olefins, transforming alcohols to carbonyl groups, for Baeyer Villager lactonization of cyclic ketones, and in other types of oxidations. It is evident that these complexes are of interest for industrial applications.

We have chosen to study oxo-peroxo complexes of Mo(VI) and V(V) with nicotinic and aspartic acid heteroligands. It is of great interest to study the interaction of three biologically important species, the metal, the peroxo group, and the bioligand. These complexes may also possess catalytic properties.

The thesis is presented in five sections. The first section consists of an introduction to the work. The second section consists of a general overview of the peroxo chemistry of V(V) and Mo(VI). The third section consists of results and discussion of the original research. The fourth section outlines the experimental procedures used and the fifth section consists of conclusions drawn from the study.

2.0. Review of the Literature

2.1. Peroxo Chemistry of Mo(VI) and V(V)

2.1.1. Peroxo Chemistry of Mo(VI)

Molybdenum has a wide range of oxidation states, ranging from -2 to +6. It has the $4d^5$ $5s^1$ electronic configuration in the ground state, and displays a variety of coordination numbers and stereochemistries as shown in Table 1.[1]

Various molybdenum oxides are known. The best known are MoO_3 and MoO_2 but other nonstochiometric oxides exist and have been studied. MoO_3 is obtained by heating Mo in oxygen. MoO_3 is a white solid which dissolves in base but not in acid. MoO_2 is formed by reduction of MoO_3. It is a brown-violet solid that dissolves in concentrated HNO_3. Several nonsto-chiometric oxides of the form MoO_x with 2<x>3 are easily formed by heating MoO_3 with Mo at ~700 C. These nonstochio-metric compounds are blue or purple.

An important part of molybdenum chemistry is its chemistry in aqueous solution. Simple molybdates are formed by

dissolution of MoO_3 solutions of alkali metal hydroxides. The molybdates obtained from these solutions are of the form $M^I_2MoO_4$ and contain the tetrahedral ion MoO_4^{-2}. As basic solutions of MoO_4^{-2} are acidified, the solution chemistry becomes much more complex. As acid is added the following equilibria are observed:

$$MoO_4^{2-} + H^+ \rightleftharpoons HMoO_4^-$$

$$HMoO_4^- + H^+ + 2H_2O \rightleftharpoons Mo(OH)_6$$
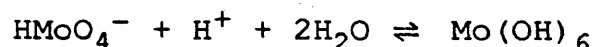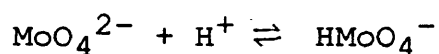
As the solution becomes more acidic, polynuclear species known as isopolymolybdates form. No polynuclear species exist with fewer than seven molybdenum atoms. This first isopolymolybdate is formed by the following reaction:

$$7MoO_4^{2-} + 8H^+ \rightleftharpoons Mo_7O_{24}^{6-} + 4H_2O$$
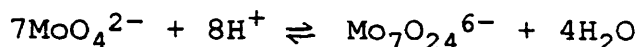
At more acid pH's, the following reaction occurs:

$$Mo_7O_{24}^{6-} + 3H^+ + HMoO_4^- \rightleftharpoons Mo_8O_{26}^{4-} + 2H_2O$$
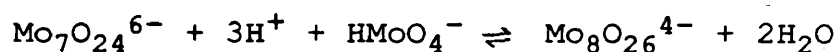
The $[Mo_6O_{19}]^{2-}$ species exists in the solid state but is not present in measurable quantities in solution. The isopolymolybdates mentioned previously also exist in the solid state. Heteropoly anions can also be formed by either acidifying solutions containing the desired anions, or by adding the heteroelement to the acidified solution.[1]

The known peroxides of molybdenum are obtained from the Mo(VI) state. Peroxo:Mo(VI) ratios of 4:1, 3:1, 2:1, 1:1, and non-integral ratios have been found as alkali and alkaline

Table 1(1)

Oxidation State	Coordination Number	Geometry	Examples
Mo^{-II}, W^{-II}	5	?	[Mo(CO)$_5$]$^{2-}$
Mo^0, W^0, d^6	6	Octahedral	W(CO)$_6$, py$_3$Mo(CO)$_3$, [Mo(CO)$_3$I]$^-$, [Mo(CN)$_5$NO]$^{4-}$ Mo(N$_2$)$_2$(diphos)$_2$
Mo^I, W^I, d^5	6^a	π-Complex	(C$_6$H$_6$)$_2$Mo$^+$, h^5-C$_5$H$_5$MoC$_6$H$_6$
	7^a		[h^5-C$_5$H$_5$Mo(CO)$_3$]$_2$
	6	?	MoCl(N$_2$)(diphos)$_2$
Mo^{II}W^{II}, d^4		π-Complex	h^5-C$_5$H$_5$W(CO)$_3$]$_2$
	5	See text	[MoCl(N$_2$)(diphos)$_2$
	6	Octahedral	Mo(diars)$_2$X$_2$,Mo(CO)$_2$(diars)I$_2$
	7	?	[Mo(diars)$_2$(CO)$_2$X]$^+$,[Mo(CO)$_2$(diars)Br$_2$]
	9	Cluster Compounds	Mo$_6$Cl$_{12}$,W$_6$Cl$_{12}$
Mo^{III},W^{III},d^3	6	Octahedral	[Mo(NCS)$_6$]$^{3-}$,[MoCl$_6$]$^{3-}$,[W$_2$Cl$_9$]$^{3-}$
	7	?	[W(diars)(CO)$_3$Br$_2$]$^+$
Mo^{IV},W^{IV},d^2	8^a	π-Complex	(h^5-C$_5$H$_5$)$_2$WH$_2$,(h^5-C$_5$H$_5$)$_2$MoCl$_2$
	9^a	π-Complex	(h^5-C$_5$H$_5$)$_2$WH$_3$
	4	Dist. tetrahedral	Mo(NMe$_2$)$_4$
	6	Octahedral	[Mo(NCS)$_6$]$^{2-}$, [Mo(diars)$_2$Br$_2$]$^{2+}$ WBr$_4$(MeCN)$_2$,MoOCl$_2$(PR$_3$)$_3$
	6	Trigonal Prism	MoS$_2$
	8	Dodecahedral or square antiprism	[Mo(NCS)$_6$]$^{4-}$, [W(CN)$_8$]$^{4-}$ Mo(S$_2$CNMe$_2$)$_4$, W(8-quinolinolate)$_4$^{b}
Mo^V,W^V, d^1	5	tbp	MoCl$_5$(g)
	6	Octahedral	Mo$_2$Cl$_{10}$(s), [MoOCl$_5$]$^{2-}$, WF$_6^-$
	8	Dodecahedral or square antiprism	[Mo(CN)$_8$]$^{3-}$, [W(CN)$_8$]$^{3-}$
Mo^{VI}, W^{VI}, d^0	4	Tetrahedral	MoO$_4^{2-}$, MoO$_2$Cl$_2$, WO$_4^{2-}$, WO$_2$Cl$_2$
	5?	?	WOCl$_4$, MoOF$_4$
	6	Octahedral	MoO$_6$,WO$_6$ in poly acids, WCl$_6$, MoF$_6$m [MoO$_2$F$_4$]$^{2-}$, MoO$_2$(distorted), WO2(distorted)
	7	Distorted pentagonal bipyramid	WOCl$_4$(diars), K$_2$[MoO(O$_2$)ox]
	8	?	MoF$_8^{2-}$, WF$_8^{2-}$
	9	?	WH$_6$(Me$_2$PhP)$_3$

^{a} If C$_6$H$_6$ and h^5-C$_5$H$_5$ occupy three coordination sites.

^{b} W.D. Bonds, Jr. and R. D. Archer, *Inorg. Chem.*, 1971, 10, 2057.

earth metal salts. There is usually uncertainty as to the degree of polymerization in the non-stochiometric ratios but it is known that the presence of H_2O_2 reduces the extent of polymerization.[2]

For the 4:1 species, $Mo(O_2)_4^{2-}$, red salts of Na^+, K^+, Ca^{++}, SN^{++}, Ba^{++}, Co^{++}, and $Zn(NH_3)_4^{2+}$ have been obtained from the addition of H_2O_2 to neutral or slightly alkaline solution of MoO_4^{2-} in the presence of the desired cation. These 4:1 peroxy species are extremely unstable. They explode when struck or warmed. $K_2Mo(O_2)_4$ gives a deep red solution in water which slowly turns yellow while evolving oxygen but at pH > 7 the $Mo(O_2)_4^{2-}$ ion is stable in excess H_2O_2 while at strongly basic pH decomposition to the MoO_4^{2-} ion occurs.[2]

For the 3:1 species, $Mo(O)(O_2)_3^{2-}$, $CaMoO(O_2)_3$ and $SrMoO(O_2)_3$ have been synthesized through thermal decomposition of their tetraperoxy counterparts. The 3:1 peroxymolybdates are brick red and thermally unstable at room temperature.[2]

For the 2:1 species, $MoO_2(O_2)_2^{2-}$, alkali metal salts of the form $M_2^I[(O_2)_2Mo(O)\ OMo(O)(O_2)_2]$ have been prepared from acidic solutions which contain alkali metal molybdates and excess H_2O_2.[2]

For the 1:1 peroxy species, $MoO_3(O_2)^{2-}$, salts of the form

M_2^I or $M^{II}[MoO_3(O_2)]*H_2O$ have been obtained by decomposition of

peroxymolybdates with more peroxo and by other methods.[2]

Several heteroligand Mo(VI) peroxo complexes have been

prepared and studied. The peroxo in these complexes is bound

in a side-on fashion. It can be considered to occupy either

one or two coordination sites, but is usually thought to

occupy two. In oxo-peroxo complexes, the oxo and peroxo

groups are almost invariably found cis to each other. This

allows maximum pi donation by the oxo and peroxo groups into

the d orbitals of molybdenum.[3]

Covalent compounds of the form $MoO(O_2)_2LL'$ have been

prepared by adding ligand to a solution of MoO_3 in H_2O_2. The

ligands used include tertiary amides, phosphoramides, amine

oxides, phosphine oxides, arsine oxides, aromatic amides, and

pyridine-2-carboxylic acid.[4]

Some novel peroxo heteroligand compounds of the form

$M^I[MoO(O_2)_2L]*H_2O$ with L = citrato, and $[MoO(O_2)_2AA]*H_2O$ with

AA = glycine, valine, or proline have been prepared by C.

Djodjevic et al.[31] These complexes are crystalline and

stable.[31] Furthermore, a Mo(VI)-oxalato complex of the form

$K_2[MoO(O_2)_2(C_2O_4)]$ has been prepared.[32] The complex is a

distorted pentagonal bipyramid with the two peroxo groups and

one of the carboxylate groups being found in the equatorial

plane and the oxo group and other carboxylate group are found

in the apical positions.[32]

Molybdenum peroxo complexes are of interest as catalysts for oxidations. These complexes have been used for oxidizing olefins, to transform alcohols to carbonyl groups, for Baeyer Villager lactonization of cyclic ketones, and in other types of oxidations.[4]

2.1.2. Peroxo Chemistry of V(V)

Vanadium has a wide range of oxidation states, ranging from -1 to +5. Its electronic configuration in the ground state is $3d^3 4s^2$. Vanadium has a variety of coordination numbers and stereochemistries as shown in Table 2.[1]

Several oxides of vanadium are known, including V_2O_5, VO_2, V_2O_3, and other nonstochiometric ratios. V_2O_5 is the most common of the oxides. It is an orange powder that dissolves in either acids or bases. VO_2 is a dark blue compound that is prepared by mild reduction of V_2O_3. It is soluble in both acid and base. V_2O_3 is a black compound also obtained by reduction of V_2O_5. It has a tendency towards oxygen deficiency and is soluble only in acid.

The aqueous chemistry of V(V) is complex and highly dependent on pH and concentration as outlined in Figure 1.[5] At pH > 13, VO_4^{3-} is the major species present in solution. As

Table 2

Oxidation States and Stereochemistry of Vanadium

Oxidation State	Coordination Number	Geometry	Examples
V^{-I}	6	Octahedral	$V(CO)_6^-$, $Li[V(bipy)_3]\cdot 4C_4H_8O$
V^0	6	Octahedral	$V(CO)_6$, $V(bipy)_3$, $V[C_2H_4(PMe_2)_2]_3$
	7	?	$V(CO)_6AuPPh_3$
V^I, d^4	6	Octahedral	$[V(bipy)_3]^+$
		Tetragonal pyramidal	$h^5\text{-}C_5H_5V(CO)_4$
V^{II}, d^3	6	Octahedral	$[V(H_2O)_6]^{2+}$, $[V(CN)_6]^{4-}$
V^{III}, d^2	3	Planar	$V[N(SiMe_3)_2]_3$
	4	Tetrahedral	$[VCl^4]^-$
	5	tbp	$trans\text{-}VCl_3(SMe_2)_2$, $VCl_3(NMe_3)_2$
	6^a	Octahedral	$[V(NH_3)_6]^{3+}$, $[V(C_2O_4)_3]^{3-}$, VF_3
V^{VI}, d^1	4	Tetrahedral	VCl_4, $V(NEt_2)_4$, $V(CH_2SiMe_3)_4$
	5	Tetragonal pyramidal	$VO(acac)_2$
		?	$[VOCl_2$ $trans\text{-}(NMe_3)_2$
		tbp	$VOCl_2$ $trans\text{-}(NMe_3)_2$
	6^a	Octahedral	$VO_2(rutile)K_2VCl_6$, $VO(acac)_2py$
	8	Dodecahedral	$VCl_4(diars)_2$
V^V, d^0	4	Tetrahedral (C_{3v})	$VOCl_3$
	5	tbp	$VF_5(g)$
		spy	$CsVOF_4$
	6^a	Octahedral	$VF_5(s)$, VF_6^-, V_2O_5 (very distorted, almost tbp with one distant O); $[VO_2ox_2]^{3-}$
	7	Pentagonal bipyramidal	$VO(NO_3)_3\cdot CH_3CN^b$

a Most important states.

b Contains both mono- and bi-dentate NO_3 groups (F.B.W. Einstein et al., *Inorg. Chem.*, 1971, 10, 678).

Figure 1 (5)
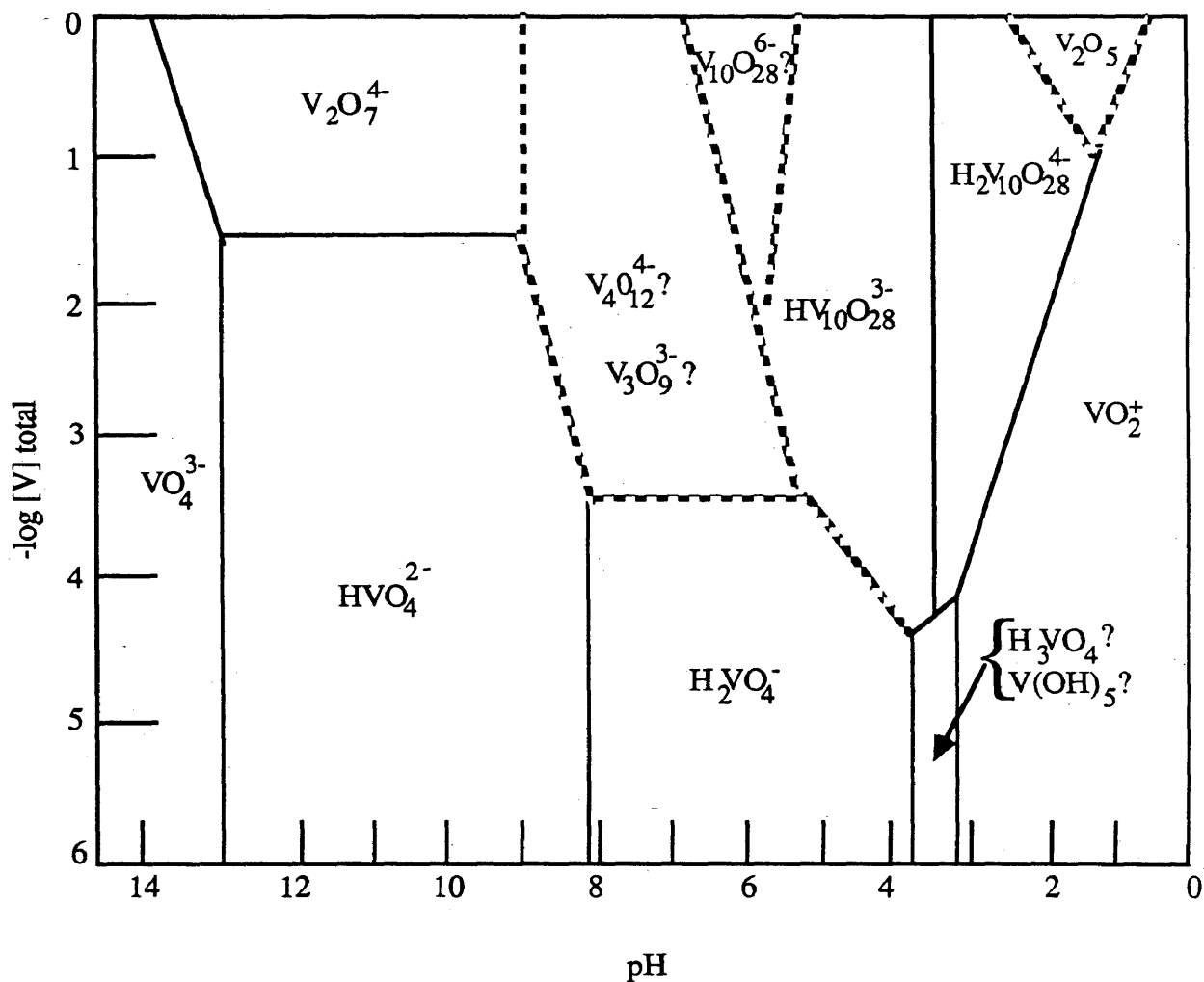
The approximate conditions of pH and total vanadium concentration under which a given species would be the major solute component of a vanadate solution at 25 C. Demarcation lines about which there is doubt are dashed.

the solution becomes more acidic, there is less certainty as to which species are present and in what concentrations. In the pH range from 2-6, the orange decavanadate ion, $V_{10}O_{28}^{6-}$ is the major species present. It can exist in several proto-nated forms such as $V_{10}O_{27}(OH)^{5-}$, $V_{10}O_{25}(OH)_3^{3-}$, $V_{10}O_{25}(OH)_4^{2-}$ and $V_{10}O_{25}(OH)$. $V_{10}O_{25}(OH)_4^{2-}$ is unstable and if further acid is present decomposes to the VO_2^+ ion.[1]

As does molybdenum, vanadium forms peroxo complexes with V:O ratios of 4:1, 3:1, 2:1, and 1:1. Salts of the tetra-peroxy species, $V(O_2)_4^{3-}$, are obtained by adding a concentrated solution of V_2O_5 in H_2O_2 at temperatures below $0°$ C. The salt is of the form $M^I_3V(O_2)_4$ with vanadium in the +5 oxidation state. This species is stable only in the presence of excess H_2O_2.[2]

The 3:1 peroxy species $VO(O_2)_3^{3-}$ is present under condi-tions of excess H_2O_2 as $H[VO(O_2)_3]^{-2}$. If excess H_2O_2 is not present, hydrolysis to a 2:1 peroxy species occurs. Addition of base to the tetraperoxy species produces the triperoxy species.[2]

The 2:1 peroxy species, $[VO(O_2)_2]^{-1}$ and $[VO_2(O_2)_2]^{3-}$, are produced by addition of excess H_2O_2 to V_2O_5. There is some uncertainty as to which of the anions listed above is the real

representation of the 2:1 peroxy species. Potentiometric titration of V_2O_5 in H_2O_2 against LiOH indicates $[VO_2(O_2)_2]^{3-}$ while the addition of an alkali hydroxide of a solution of V_2O_5 in H_2O_2 results in the precipitation of $M^IH_2[VO(O_2)_2]$. An equilibrium between $[VO(O_2)_2]H_2O$ and $[VO_2(O_2)_2]^{3-}$ has been suggested.[2]

The 1:1 peroxyvanadate, $[VO(O_2)]^+$, can be prepared by several methods, the most obvious of which is addition of H_2O_2 to V_2O_5. The 1:1 peroxyvanadate produces a red color in solution and is stable under moderately acid conditions.[2]

Several novel oxo-peroxo vanadium complexes with various heteroligands that contribute to the stability of the complexes have been prepared. The complexes that have been studied are either mono or diperoxo. Monoperoxo complexes that have been prepared are as follows:

$Na_3[VO(O_2)EDTA]*4H_2O$[34], $K[VO(O_2)_2(dipic)]*2H_2O$[35],

$H[VO(O_2)(dipic)H_2O]*H_2O$[35], $[VO(O_2)Pic]*2H_2O$[37],

$NH_4[VO(O_2)(H_2O)(C_5H_3N(COO)_2]*xH_2O$[39] with x~1.3, and
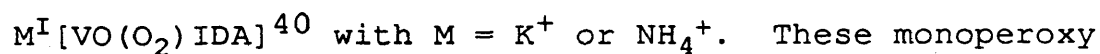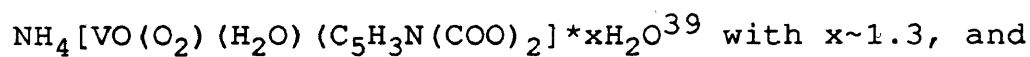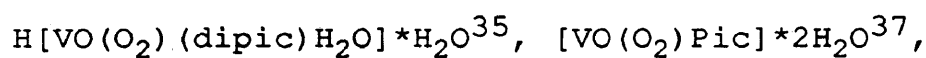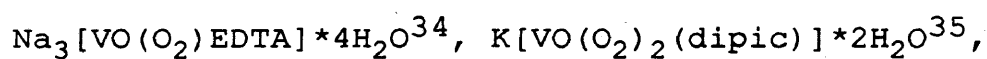
$M^I[VO(O_2)IDA]$[40] with $M = K^+$ or NH_4^+. These monoperoxy complexes are 7-coordinate with coordination geometry being either a pentagonal bipyramid or a distorted pentagonal bipyramid. Diperoxo compounds that have been synthesized and

studied are as follows: $K_3[VO(O_2)_2(C_2O_4)]*H_2O^{38}$,

$M[VO(O_2)_2*nH_2O^{36}$ with $M = Na^+$, K^+, or NH_4^+, and

$M_3[VO(O_2)_2(ox)]*2H_2O^{36}$ with $M = K^+$ or NH_4^+. The structure of

$K_3[VO(O_2)_2(C_2O_4)]*H_2O$ has been done and it has been shown

to be a 7-coordinate pentagonal bipyramid.[38] Two peroxo

groups and an oxalato group oxygen form the pentagonal plane

while the oxo ligand and another oxalato group oxygen occupy

and apical positions.[38]

2.2. Metal Complexes of the Alpha Amino Acids

There are twenty alpha amino acids that commonly occur in

proteins. Amino acids all have the same general form, con-

taining an amino group, a carboxylate group, and an R-group,

all of which are bound to the same carbon atom. Each is

characterized by its unique R-group. Alpha amino acids are

biologically important as they are the building blocks for

peptides and proteins. Metal complexes of amino acids are of

interest because of their role in biochemistry. Metals are

essential in the function of many enzymes, oxygen transport,

and electron transport. The study of complexation of amino

acids with metals is a first step towards understanding the

biochemistry of metals that are essential for life. Metal-

amino acid complexes also serve as models for protein-metal

binding.

Amino acids can bind to metals through the nitrogen of the alpha amino group, through the oxygen(s) of the carboxylate group, or through some R-groups. Chelation of the amino acid to the metal is important due to the favorable entropy effects.

Coordination of the carboxylate moiety to the metal can occur in five distinguishable ways as shown in Figure 2.[6] In type a, the metal is bound to a single oxygen atom. In type b, a second metal atom binds weakly to the free carboxylate oxygen. In type c, two metal atoms bind equally to each carboxylate oxygen. In type d, one metal atom binds unequally to each oxygen, and in type e, a single metal atom binds equally to each carboxylate oxygen. Chelation is present in types d and e with the carboxylate group acting as a bidentate ligand. Carboxylate binding as in types b and c is frequently found in crystal structures. These two types of binding contribute to the stability of dimeric and polymeric complexes in solution.[6]

Despite their high pKa values, amino group binding is common. This is due to the strong electron donating character of nitrogen, and to the fact that chelation with a carboxylate oxygen can easily occur to form a favored five-member ring.[6]

Alpha amino acids can be separated into three groups according to the properties of their R-group. There are amino acids with "hard" donor centers contained within the R-group. Examples are serine and aspartic acid. There are amino acids

with "soft" donor centers in their R-groups such as histidine and penicillamine. And, of course, there are amino acids with non-coordinating R-groups.[7]

Amino acids that contain "hard" donor centers in their R-groups range from the hydroxyl groups contained in serine, threonine, and tyrosine, to the carboxylate groups contained in aspartic and glutamic acid, and to the amino group contained in lysine.[7]

The extent of coordination of the side chain hydroxyl groups is uncertain.[6,7] However, it appears that in most cases the hydroxyl groups do not interact with the metal. A metal hydroxyl interaction has been observed for Zn(L-Ser) at pH = 12, but the hydroxyl group is interacting with the neighboring Zn atom of a polynuclear species and is not considered important.[6]

The coordination of carboxylate groups and amino groups were discussed above. There is no difference in the way these groups coordinate as a part of the side chain, but the proximity of alpha amino and alpha carboxylate groups for chelation may be different.

Amino acids that contain "soft" donor centers in their R-groups range from amino acids such as methionine, cysteine, and penicillamine, to histidine. Methionine, cysteine, and penicillamine contain a sulfur atom while histidine contains an imidazole nitrogen.[7]

Figure 2 (6)

(a) (b) (c) (d) (e)
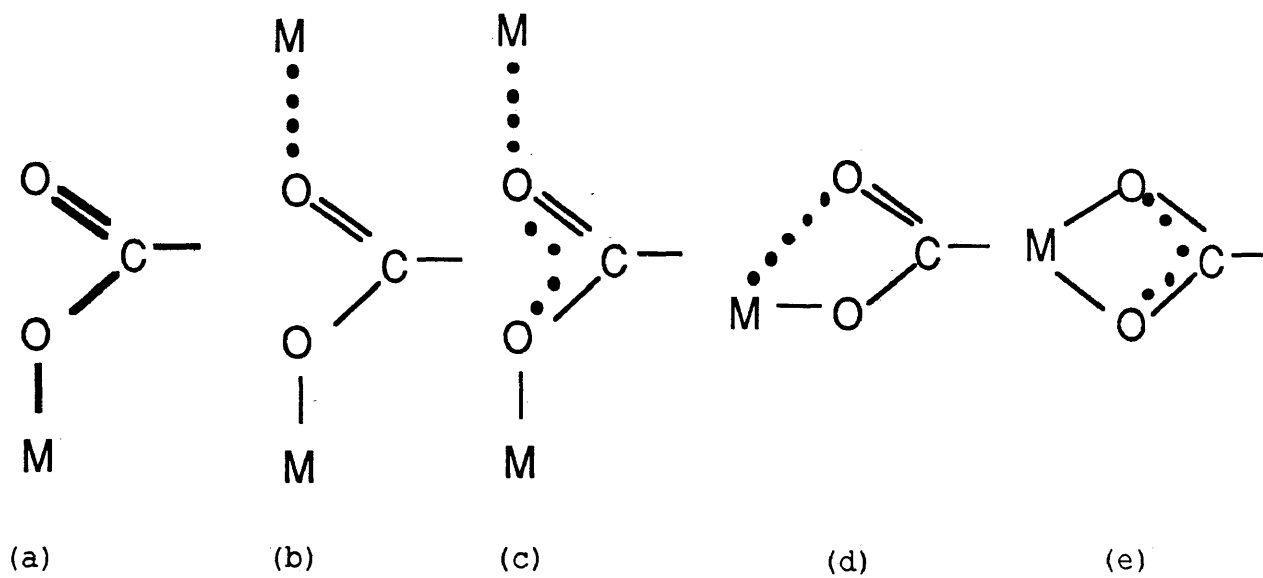
O (carboxyl)-metal interactions

Certain metals have a high affinity for sulfur as a ligand. These are metals that form strong sigma bonds with polarizable ligands and form pi bonds by donation of electrons from the metal's d-orbitals to the ligands d- or p-orbitals. These sulfur containing amino acids complex with many metals, especially those in a triangular area near the center of the periodic table. Unidentate, bidentate, and tridentate chelation has been found.[6]

Histidine has two potential binding sites in its R-group. These imidazole nitrogens are referred to as the imidazolium nitrogen and the imidazole nitrogen. The imidazolium nitrogen has a pKa of ~6 while the imidazole nitrogen has a pKa of ~14.[6] Binding of the imidazole nitrogen is of great interest because it is one of the major ways that metals bind to proteins.[8] Histidine can bind to metals that tend to form octahedral complexes in a tridentate manner, but this occurs only at higher pH's.[8] At lower pH's histidine binds as a bidentate ligand.[8]

2.3. Metal Complexes of Nicotinic Acid

Nicotinic acid (3-pyridine carboxylic acid) is a vitamin more commonly known as niacin. Its structure is shown in Figure 3. Nicotinic acid (NAH) has two potential binding sites, the carboxylate group oxygens and the pyridine nitrogen. Its structure and binding properties are similar to those of the alpha amino acids.

Metal complexes with NAH have been reported for chromium, manganese, iron, cobalt, nickel, copper, zinc, silver, cadmium, germanium, and lanthanum. Several modes of coordination for NAH have been reported in the literature. In complexes of the form [M(II)NA$_2$*4H$_2$O] with M(II) = Co, Zn, Ni, Cr, or Mn, NA binds through its pyridine nitrogen while in the tetra and pentahydrates with M = Cr(III) coordination of NA occurs through the carboxylate group.[10] However, some anhydrous complexes of this type with M = Mn-Zn and Ag are binuclear or polynuclear with NA serving as a bridging ligand and coordinating through its pyridine N and one of its carboxylate oxygens.[9] NAH serves as a chelating ligand in Cd(II)NA$_2$ with chelation occurring through both carboxylate oxygens.[9] Ge(IV)Cl$_2$NA$_2$ was found to have chelation occurring through the pyridine N and one of the carboxylate oxygens.[9]

Complexes of the form [M(N-NAO)$_2$(OH)$_2$]n*H$_2$O have been synthesized for M = Mn-Zn with m = 2n for Mn-Cu and m = 3n for Zn. Coordination is thought to occur through the N-O oxygen and through one of the carboxylate oxygens with the free carboxylate oxygen being bound to water. The complexes are hexacoordinated and polynuclear.[9]

Several Cr-NAH complexes have been reported. These complexes are of particular interest since Cr-NAH complexes have been associated with glucose metabolism.[11,12] Complexes

Figure 3
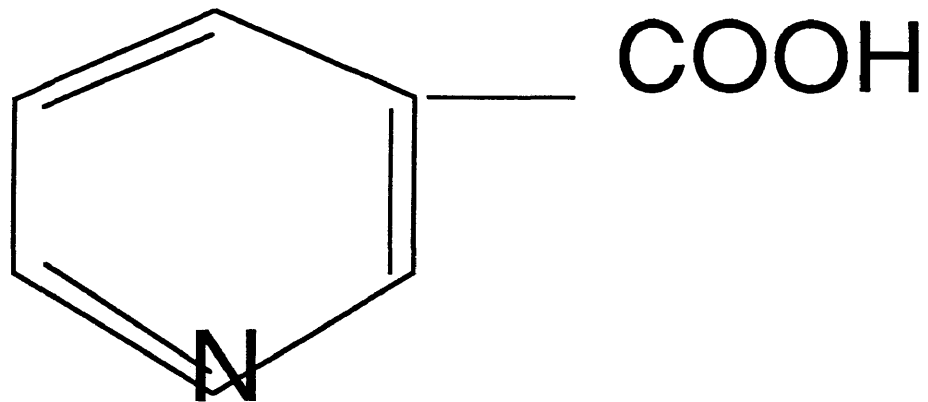
Nicotinic acid
(niacin)

Figure 4
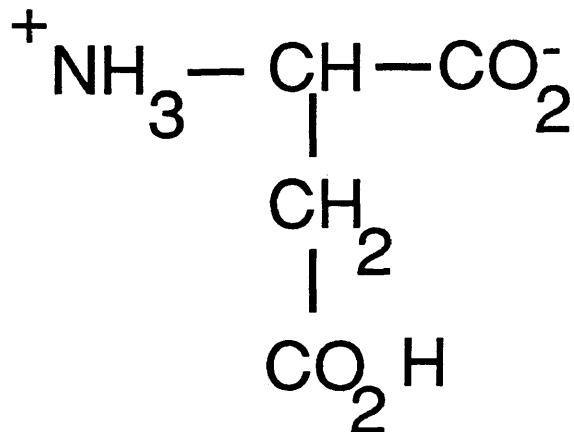
Aspartic Acid

of the form $[Cr(III)NA_2]^+*(H_2O)_4$, $[Cr(III)NA_2]^{2+}*(H_2O)_5$, and

$[Cr(II)NA_2]*(H_2O)_4$ have been prepared.[10] Coordination through

one of the carboxylato oxygens is evident for the Cr(III)

complexes while complexation through the pyridine nitrogen

occurs in the Cr(II) complex. It appears that trans

coordination of the two NA ligands occurs for each of the

three complexes.[10] Biological activity was observed only for

the O-coordinated complexes.[10]

Several Cr(III)-NAH complexes have been prepared by Chang

et al. in an effort to explore the biological activity of

Cr(III)-NA complexes. The complexes prepared are the

following: $[CrNA(NH_3)_5](ClO_4)_2$, cis-$[Cr(NA)_2(HN_3)_4]ClO_4$,

cis-$[Cr(NA)_2(NH_3)_4]Br$, trans-$[Cr(NA)_2(NH_3)_4]ClO_4$, and

cis-$[Cr(NA)_2(en)_2]Br$. Coordination through a carboxylato

oxygen was observed for each complex.[12]

The complex $[Cr(salen)(NA)H_2O)]$ has been prepared and

studied. Coordination occurs through one of the carboxylato

oxygens.[13]

The complex trans-$[Cr(1,3-pn)_2(NA-O)_2]Cl*4H_2O$ has been

prepared and studied. It is the first Cr(III)-NAH complex

that is stable at physiological pH. Coordination of the NAH

occurs through one of the carboxylato oxygens and the

stability of the complex is attributed to the chelation of the

1,3-propanediamine.[14]

The first N-coordinated Cr(III)-NAH complexes that are stable for several hours at physiological pH have been reported. These complexes are cis and trans-H[Cr(mal)$_2$(NA)$_2$]. The pyridine nitrogen has an affinity for Cr(II) so the complex was synthesized with Cr(II) as a starting material with later oxidation to Cr(III). The cis and trans assignments were made through the use of UV-Vis spectra and comparison with the UV-Vis spectra of trans-Li[Cr(mal)$_2$(py)$_2$].[15]

A trinuclear Cr(III)-NA complex of formula Na[Cr$_3$O(NAH)$_6$(H$_2$O)$_3$][ClO$_4$]$_8$*NAH*6H$_2$O has been prepared and studied. The three CR's are each bound to a central oxygen atom. The NA zwitterions form bridges between the Cr's through their carboxylato oxygens. A water molecule on each Cr is located trans to the central oxygen. The coordination of each Cr atom is octahedral.[16]

Several Cu(II)-NAH complexes have also been prepared and studied. Complexes of the form [L$_3$ClCuL$_2$CuClL$_3$]Cl$_2$ have been sythesized with L = NA N-oxide. Coordination, of both a terminal and bridging nature, occurs only through the N-oxide oxygen.[17]

A similar Cu(II) complex, [CuCl$_2$(N-NAOH)$_2$], has been prepared. The coordination of the complex is distorted square planar and coordination of NAH occurs through the N-oxide oxygen. Two carboxylato oxygens of adjacent molecules complex

with the Cu(II) from long distances to complete the coordination sphere.[18]

Another polymeric Cu(II)-NA complex of the form {[Cu(N-NAO)$_2$(H$_2$O)$_2$]*4H$_2$O]}n has been synthesized. The NA-N-oxide ligands are bidentate. These ligands form bridges between adjacent Cu's with coordination occurring through one of the carboxylato oxygens and through the N-oxide oxygen. Coordination is that of an elongated octahedron. The complex is unstable.[19]

Another polymeric Cu(II)-NA-N-oxide complex of the form [Cu$_3$(NA-N-O)$_4$(OH)$_2$(H$_2$O)$_2$]n has been prepared and studied. NA-N-oxide serves as a bridging ligand with bidenatate coordination occuring through both carboxylato oxygens as between Cu1 and Cu2(2') or bidentate coordination occurring through one carboxylato oxygen and one N-oxide oxygen as between Cu2 and Cu2' where a double bridge occurs. The complex is a polymeric, linear chain whose tricopper structural units are connected through two N-oxide oxygens. The coordination of Cu1 is square planar while the coordination of Cu2(2') is distorted square planar.[20]

A few complexes of cobalt and nickel with NA have been prepared. Complexes of the form [M(NA-N-O)$_2$(H$_2$O)$_4$] with M = Co(II) or Ni(II) have been synthesized. Coordination of the ligand to the metal occurs through one of the carboxylato oxygens for each ligand. The NA-N-oxide groups are trans to

each other and the coordination geometry is a slightly
distorted octahedron.[21]

2.4. Metal Complexes of Aspartic Acid

Aspartic acid (Asp) is one of the twenty alpha-amino acids
commonly found in proteins. Its structure is shown in Figure
4. Its R-group consists of CH_2COO- so there are three possible
sites for coordination to the metal. Aspartic acid is usually
tridentate forming 5, 6, and 7-membered chelate rings.[7]

Complexes with aspartic acid have been prepared for the
following metals: magnesium, calcium, strontium, barium,
zinc, cadmium, cobalt, nickel, copper, chromium, molybdenum,
platnium, palladium, and uranium. Limited work has been done
on complexes of Asp with second and third row transition
metals due to easy hydrolysis and/or kinetic inertness.[7]

Little has been reported on the complexation of Mo due to
the fact that the stable MoO_4^{2-} species predominates at basic
pH while isopolymolybdates predominate at acidic pH.
Complexation is best studied near pH = 6.[7] The formation of
$[MoO_3Asp]^{2-}$ has been reported by Rabenstein et al.[22] The
coordination of the ligand is thought to be tridentate.[24] The
complex $K_2[MoO_3Asp]*H_2O$ has been reported by Butcher et al.[23]
In this complex the oxo groups were found to be cis to each
other and the Asp ligand is tridentate.[23]

Cu(II)-Asp complexes have been reported both with and without mixed ligand coordination spheres. Complexes of the form CuL and CuL_2^{2-} form with L=Asp.[7] The coordination of Asp is not certain in these complexes.[7] $K_2[CuAsp_2]*H_2O$ has been prepared.[27] Tridenatate coordination is presumed since there is only a single absorption in the carbonyl region which is consistent with metal coordinated carboxylato groups.[7] Two mixed ligand Cu(II)-Asp complexes and a single ligand Cu(II)-Asp complex have been prepared.[25, 26] The single ligand complex is of the form [CuAsp]*2H_2O and its mixed complex is of the form [CuAspB]*xH_2O with x = 2 when B = imidazole or morpholine, x = 1 when B = 2-methylimidazole, and x = 0 when B = pyridine or 4-methylpyridine.[26] The x-ray structure was done for [CuAspIm]*2H_2O.[26] It was found that the structure consists of three Cu atoms in which each Cu atom coordinated to three aspartates and one imidazole and the coordination of each Cu atom is that of a distorted square pyramid.[26] Coordination of the Asp occurs through the alpha carboxylato group and through the carboxylato group contained within the R-group.[26] The alpha carboxylato group binds to two different Cu atoms through its oxygens while the R-group carboxylato binds through one of its oxygens to a third Cu atom.[26] Similar structures are proposed for the other complexes of the same general form with the exception of those

with B = 4-methyl- pyridine or the monoligand complex.[26]

Another mixed ligand Cu(II)-Asp complex has been prepared and studied. This complex has the molecular formula [CuAsp bpyH$_2$O]*3H$_2$O with bpy = bipyridine. The x-ray structure was done for the complex and it was found that the coordination around the Cu atom is that of a 5-coordinated distorted square pyramid. The copper atom is bound to the two nitrogens of bipyridine, one O of the alpha carboxylato group of Asp, and to the alpha-amino group of Asp within the plane. The water molecule is bound out of the plane.[25]

Ni(II)-Asp complexes have been prepared and a mixed ligand complex with imidazole has also been prepared as was done for Cu.[29] A complex of the form [NiAsp(H$_2$O)$_2$]*H$_2$O has been prepared and studied.[28] This complex is isostructural with corresponding Zn(II) and Co(II) salts.[28] The complex is linear polymeric and the coordination of Ni is that of a distorted octahedron.[28] Coordination occurs with bonds to the alpha amino, alpha carboxylato, and R-group carboxylato groups of one Asp which is functioning as a tridentate ligand.[28] The coordination sphere is completed by two water molecules and the R-group carboxylato oxygen of a second aspartate molecule that is also bound to another Ni atom.[28]

Some Cr(III) complexes of the forms [CrAsp$_2$] and [CrAspHis] have been prepared. Tridentate coordination of both ligands is observed with the aspartate ligands being

coordinated through an alpha carboxylato oxygen atom, a R-group carboxylato atom, and the alpha amino nitrogen. Octahedral coordination is observed and it is noted that amino groups avoid being trans to each other in both complexes.[30]

Complexes of zinc and cadmium with aspartate have been prepared. They are of the forms ML and ML_2^{2-}. Aspartate is throught to be tridentate in these complexes. In addition to these complexes the structure of $[ZnAsp(H_2O)_2]*H_2O$ has been done and it is seen that the Asp is tridentate and coordination of the complex is octahedral.[7]

Pd(II) forms 1:1 and 1:2 complexes with Asp. Coordination is bidentate and the coordination geometry is square planar. Pt(II) has been shown to have both mono and bidentate coordination with Asp and forms complexes of the forms PtCl Asp and PtAsp. The side chain carboxylato group does not coordinate to the metal.[7]

Little has been reported on complexation of magnesium, calcium, strontium, and barium but it appears that binding of the Asp ligand to these metals is either mono or bidentate. Similarly, little has been reported on complexation of the lanthanides and actinides but it has been shown that uranium coordinates to Asp through the carboxylato groups.[7]

3.0. Results of the Original Work and Discussion

3.1. Peroxo Complexes with Nicotinic Acid(NAH)

Mo(VI) and V(V) peroxo systems with NAH in aqueous media were studied in order to find out if the three biologically important species: the metal ion, the peroxo group and the NAH combine, forming interesting complexes. It has been found that such interactions indeed can occur, and we have prepared the first complexes where peroxo groups are present in combination with a NAH group in one ligand sphere. Mo(VI) and V(V) differ in their behavior, as described below.

3.1.1. Mo(VI) Complexes

Three molybdenum peroxo complexes with nicotinic acid have been prepared and studied. These yellow, diperoxy complexes represent new compounds which have not previously been reported in the literature. The systems we have studied consisted of aqueous Mo(VI) peroxo solutions with NAH in the absence and the presence of potassium and ammonium cations. The complexes obtained from these solutions were
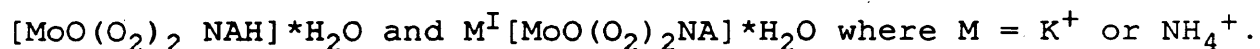
$[MoO(O_2)_2 NAH]*H_2O$ and $M^I[MoO(O_2)_2NA]*H_2O$ where $M = K^+$ or NH_4^+. They have been characterized by peroxo analysis by Ce(IV) titrations, microanalysis for C, H, and N, IR spectra, UV-V spectra, and cyclic voltametry.

Theoretical and observed values for C, H, N, and O_2^{2-} analyses are shown in Table 3. The Table shows that the theoretical and observed values for the proposed formulae correlate closely.

Infrared spectra are especially useful in revealing the presence of coordinated ligands, and the type of metal-oxo bonds. The characteristic bands are listed in Table 5 and shown in Figures 4, 5, and 6. Characteristic absorptions observed in the complexes were strong metal-oxygen stretching frequencies at ~970 and 950 cm^{-1}, strong peroxo stretching frequencies at ~875 and 858 cm^{-1}, coordinated carboxylato stretching frequencies in the region of 1600 cm^{-1}, and other absorptions that originated in the NAH. C-H and Mo-O stretching bands were also useful in characterizing the complexes, with the C-H stretches appearing as weak bands in the 3100 cm^{-1} region as shown in Figures 19-21, and the Mo-O stretches appearing as weak to medium bands in the 350 cm region. The free NAH showed a strong carboxylato absorption at 1708 cm^{-1} which was compared to strong coordinated carboxylato absorptions at 1660 cm^{-1} for [MoO(O$_2$)$_2$NAH]*H$_2$O, at 1676 cm^{-1} for the potassium salt, and at 1668 cm^{-1} for the ammonium salt. Various weaker absorptions were observed in the 1500-1700 cm^{-1} range, some of which can be attributed to carboxylato stretching. The complexes also exhibit absorptions around 3400 cm^{-1} due to OH stretching of the water

molecules present. The complexes show a weak N-H and C-H stretching frequencies near 3100 cm^{-1} as shown in Figures 19-21, and the ammonium salt shows five weak absorptions in that region. For [MoO(O$_2$)$_2$NAH]*H$_2$O these absorptions are attributed to NAH. For NH$_4$[MoO(O$_2$)$_2$NA]*H$_2$O, these absorptions originate in the ammonium cation and for the potassium salt of the Mo complex, a band at this frequency is attributed to C-H stretching in the pyridine ring.

UV-V spectra were done of the complexes in both the aqueous solution and the solid state. As shown in Table 6 and Figure 12, for the solid state spectra, each of the three molybdenum complexes exhibits a broad peak extending from 250 - 400 nm and a shoulder at 234 nm. The free NAH absorbs at 250 nm as shown in Figure 11. The broad peaks are attributed to charge transfer between the peroxo groups and the metal and the shoulders are attributed to slightly shifted absorptions of the NAH ligand.

UV-V spectra in the aqueous solutions were done in 0.1 M KCL as shown in Table 7 and Figure 12, and over a range of pH's in KCL/KOH/HCL solution with μ = 0.1. at concentrations of 10^{-4} - 10^{-5}M. It was necessary to use low concentrations in order to resolve the peaks. The spectra for [MoO(O$_2$)$_2$NAH]*H$_2$O were not done over a range of pH's due to difficult in dissolving the compound and due to solvent absorption at concentrations 10^{-5}M or less. In the 0.1 M KCL, as shown in Table 7, the complexes each showed an absorption

band in the 257-260 nm region and the free NAH absorbed at 262 nm (Figure 1) with ε = 3500 $M^{-1}cm^{-1}$. The Mo complex and its ammonium salt each showed an additional weaker peak at 300 nm. The absorptions of the complexes in the 257 - 260 nm range are due to the NAH present and the absorptions at 300 nm are attributed to charge transfer. The appearance of charge transfer bands is dependent upon the concentration of the solution studied. The charge transfer bands have a much lower ε value than the bands due to NAH and do not appear in every solution studied.

The pH dependence proved to be more complex, at least for K[MoO$(O_2)_2$NA]*H_2O, as shown in Table 8. For pH's 0.68-8.66, each spectrum exhibited an absorption in the 250-262 nm range. For pH's 1.17, 2.33, 2.76, 3.05 and 3.81 each exhibited an additional stronger absorption in the 205-217 nm range. For pH's of 2.33, 3.05, 2.81, 4.52, 5.90, and 6.99 each had an additional weaker absorption in the 302-308 nm range. As before, the absorptions in the 250-262 nm range are attributed to absorption of the NAH and the absorptions in the 302-308 range are attributed to charge transfer. $\bar{\varepsilon}$ values are 1200 and 170 $M^{-1}cm^{-1}$ for the NAH and charge transfer absorptions, respectively. It is evident from these data that ε differs by approximately a power of 10 between the NAH absorptions and the charge transfer absorptions.

The pH series for NH$_4$[MoO$(O_2)_2$NA]*H_2O provided a simpler picture with absorptions between 257 and 262 nm with $\bar{\varepsilon}$ =3600

for all the spectra done in the pH range 0.57-7.72. Weaker absorptions in the 300-325 nm range occurred for pH's in the 0.57-5.56 range. The absorptions near 260 nm are attributed to NA and the weaker absorptions in the 300-325 range are attributed to charge transfer.

A three cycle cyclic voltamogram was done for each complex with both forward and reverse scans. Cyclic voltametry is a technique which allows the potential range of an electrode to be scanned rapidly. When an oxidation or reduction occurs at the electrode-solution interface a current flows. This results in either an anodic or a cathodic peak. The potential of these peaks can be measured, providing us with information on the potentials where oxidations and reductions occur in the system. As shown in Tables 11 and 12, it should be noted that the peaks for each cycle and for forward and reverse scans are similar for each complex. In comparison among the three complexes, the cathodic peaks are similar but the anodic peaks differ significantly. $[MoO(O_2)_2NAH]*H_2O$ has anodic peaks for each cycle, forward and reverse, in the -200 to -260 mv range and in the 1360-1500 mv range. However, the negative anodic peaks are not indicative of a reversible couple since there is a difference of more than 58 mv between these values and the cathodic values. The potassium salt of the complex has values in the 1300-1450 mv range while the ammonium salt has values in the 1500-1770 mv range with no peak for cycles two and three in the reverse voltamogram. The results are represented in Figures 14 and 15.

Our studies show that in combination with the peroxo groups NAH can coordinate as a neutral ligand, most likely in the form of a zwitterion, or as a deprotonated NA which occurs at a higher pH. Infrared spectra indicate the presence of a coordinated carboxylato group, and the complexes may well have a seven-coordinate structure, as shown in Figure 10, found in the $[MoO(O_2)_2AA]*H_2O$ series, and some other peroxo hetero-ligand Mo(VI) complexes.

3.1.2. V(V) Complexes

One vanadium peroxo complex with NAH has been prepared and studied. This yellow, diperoxy complex represents a new compound which has not previously been reported in the literature. The system we studied consisted of an aqueous V(V) peroxo solution with NAH in the presence of potassium cations. The complex obtained was $K[VO(O_2)_2NAH]*H_2O$.

It has the same composition as two of the molybdenum complexes with V(V) replacing Mo(VI) but the chemical analyses and infrared spectra indicate the presence of a protonated nicotinato ligand. This complex has been characterized by peroxo analysis using Ce(IV) and $Na_2S_2O_3$ titrations, micro-analysis for C, H, and N, V(V) analysis deduced from $Na_2S_2O_3$ titrations, IR spectra, UV-V spectra, and cyclic voltametry.

Theoretical and observed values for C, H, N, V, and peroxide analyses are shown in Table 3. The table shows that

the theoretical and observed values correlate closely.

Infrared spectra are especially useful in showing the presence of coordinated ligands, and the V-oxo group. The characteristic bands are listed in Table 5 and shown in Figure 7. Characteristic absorptions observed in the complexes were strong metal-oxygen stretching frequencies at 975 and 944 cm^{-1}, strong peroxo stretching frequencies at 890 and 872 cm^{-1}, coordinated carboxylato stretching frequencies in the region of 1600 cm^{-1}, and other absorptions that originated in the NAH. C-H and V-O stretching bands also proved to be useful in characterization of the complex. The C-H stretching frequencies, as shown in Figure 22, occurred as two medium absorptions in the 3100 cm^{-1} region and the V-O stretching frequencies appeared as three weak absorptions in the 350 cm^{-1} region. The free NAH showed a strong carboxylato absorption at 1708 cm^{-1}, which was compared to a strong coordinated carboxylato absorption at 1740 cm^{-1} in the complex. Various weaker absorptions occurred in both the NAH and the complex in the 1600 cm^{-1} region which can be attributed in part to carboxylato stretching. The complex showed two absorptions of medium intensity near 3500 cm^{-1} which was attributed to OH stretching. The complex also shows a weak absorption at 3080 cm^{-1} and a medium absorption at 3110 cm^{-1} as shown in Figure 22, which were assigned to N-H and C-H stretching in the NAH.

UV-V spectra were done on the complex in both the aqueous solution and the solid state. As shown in Table 6 and Figure 13, for the solid state spectra, the complex exhibited a broad

peak near 360 nm and a shoulder at 230 nm. These bands are attributed to charge transfer between the metal and the peroxo groups and ligand absorption, respectively.

UV-V spectra in the aqueous solution were done in 0.1 M KCL as shown in Table 7 and Figure 13, and over a range of pH's in KCL/KOH/HCL solution with $\mu=0.1$. In the 0.1 M KCL the complex showed absorptions at 333 and 265 nm that are attributed to charge transfer and NAH absorption, respectively. In the pH dependence study, for a pH range of 0.55-7.58, an absorption occurred in the 258-263 nm range for each pH studied. Additional absorptions in the 315-325 nm range occurred at pH's = 3.18, 5.79, and 7.58. $\bar{\mathcal{E}}$ was 3000 and 95 $M^{-1}cm^{-1}$ for the NAH and charge transfer absorptions, respectively.

A three cycle cyclic voltamogram was done for the complex with both forward and reverse scans. The results of this study are shown in Table 12 and Figures 15 and 16. Three cathodic peaks are observed for each cycle, both forward and reverse, with the exception of the first forward cycle, in which a single cathodic peak is observed at -1200 mv. For the remainder of the cycles, both forward and reverse, the first two peaks are similar but the last peak occurs at -1200 mv for the first reverse cycle and between -700 and -800 for the remainder. Three anodic peaks are very similar for each cycle. There appears to be a partially reversible process in cycles two and three with potential differences of less than 58 mv between the positive cathodic peaks and the first anodic peaks.

3.2 Peroxo Complexes with Aspartic Acid (Asp)

Aspartic acid, the naturally occurring alpha amino acid, with an additional functional group as compared to nicotinic acid, is expected to act as an interesting ligand for Mo(VI) and V(V), and the presence of peroxo groups brings these systems an additional dimension. We found the aqueous systems of this type very interesting, but the separation of the solid complexes proved to be a real challenge. The results are described below.

3.2.1. Mo(VI) Complexes

The preparation of a molybdenum peroxo complex with aspartic acid has been attempted. The system we studied consisted of an aqueous Mo(VI) peroxo solution with aspartic acid in the presence of potassium cations. The substance obtained was not pure, but did contan the coordinated aspartate. Coprecipitation of the complex with potassium oxoperoxomobybdates makes it impossible to obtain the pure compound so the exact molecular formula is not known.

The substance has been characterized by peroxo analysis using Ce(IV) titrations, microanalysis for C, H, and N, IR spectra, UV-V spectra, and cyclic voltametry.

The observed values for C, H, N, and O_2^{2-} analyses are

spectra, UV-V spectra, and cyclic voltametry.

The observed values for C, H, N, and O_2^{2-} analyses are shown in Table 4. The values for C, H, and N are very low which is indicative of a mixture. The percentage of peroxide is too low to indicate a diperoxy species and too high to indicate a monoperoxy species.

The IR spectra provide us with some useful information about this complex. Characteristic absorptions observed in the complex are a strong metal-oxygen stretching frequency at 960 cm^{-1}, strong and medium peroxo stretching frequencies at 900 and 860 cm^{-1}, respectively. C-H and Mo-O stretching bands were also useful in characterizing the complex with the C-H stretches appearing as weak bands near 2900 cm^{-1} and the Mo-O stretches appearing as medium bands at 312 and 360 cm^{-1}. The free Asp showed medium carboxylato absorptions at 1690, 1650, and 1600 cm^{-1} which were compared to a strong coordinated absorption at 1605 cm^{-1}. Various weaker absorptions appeared in the 1500-1700 cm^{-1} range which can be contributed in part to carboxylato stretching. The complex also exhibits strong absorptions at 3500 and 3200 cm^{-1} which are assigned to O-H and N-H stretching, respectively. The characteristic bands are listed in Table 13 and shown in Figure 8.

UV-V spectra were done on the complex in both the aqueous solution and the solid state. As shown in Table 6, for the solid state spectra, the complex exhibits a broad peak near 357 nm and a shoulder at 230 nm. Aspartic acid does not absorb in the UV-V. These absorptions are attributed to

charge transfer between the peroxo groups and the metal.

UV-V spectra in the aqueous solution were done in 0.1 M
KCL as shown in Table 7 and over a range of pH's in
KCL/KOH/HCL solution with μ = 0.1 at concentrations of 10^{-4} -
10^{-5}M. We were unable to resolve the absorptions at every pH
studied. In the 0.1 M KCL the complex showed a single charge
transfer absorption at 290 nm. For the pH dependence series,
as shown in Table 14, a single absorption was observed at most
pH's in the 203-217 nm range with no absorptions being
observed at pH's of 0.66, 1.23, and 4.93.

A three cycle cyclic voltamogram was done for the complex
with both forward and reverse scans. The results of this
study is shown in Table 16 and Figure 14. Three cathodic
peaks are observed for each cycle, both forward and reverse
and the peaks are very similar for each cycle. For the anodic
peaks, one peak near 1300 mv is observed for each cycle, both
forward and reverse. For the second and third reverse cycles,
additional anodic peaks are observed at 970 and 870 mv,
respectively. No reversible couples are observed for the
system.

3.2.2. V(V) Complexes

One vanadium peroxo complex with Asp has been prepared and
studied. This yellow, diperoxy complex represents the first
peroxo aspartate compound and has not been previously reported
in the literature. The system we studied consisted of an

aqueous V(V) peroxo solution with Asp in the presence of potassium cations. The complex obtained was of the form $K_3[VO(O_2)_2Asp_2]$. Unlike the systems previously studied, this complex contains two heteroligands instead of one and no water. The complex has been characterized by peroxo analysis using Ce(IV) and $Na_2S_2O_3$ titrations, microanalysis for C, H, and N, V(V) analysis deduced from $Na_2S_2O_3$ titrations, IR spectra, UV-V spectra, and cyclic voltametry.

Theoretical and observed values for C, H, N, and O_2^{2-} analyses are shown in Table 11. The table shows that the theoretical and observed values for the proposed formula correlate reasonably well.

Infrared spectra are especially useful in showing the presence of coordinated ligands, and the V-oxo group in the complex. The characteristic bands are listed in Table 13 and shown in Figure 9. Characteristic absorptions observed in the complex were strong metal-oxygen stretching frequencies at 973 and 939 cm^{-1}, strong peroxo stretching frequencies at 889 and 870 cm^{-1}, coordinated carboxylato stretching frequencies in the 1600 cm^{-1} region, and other absorptions that originated in the Asp, C-H and Mo-O stretching frequencies were also useful in characterization of the complex, occurring at 2925 and 359 cm^{-1}, respectively. The free Asp showed absorptions of medium intensity at 1690, 1650, and 1600 cm^{-1} while the coordinated carboxylato shows absorptions of medium intensity at 1690, 1650, and 1608 cm^{-1}. The similarity of these absorptions

creates some doubt as to whether the Asp is coordinated through one of its carboxylato groups and introduces the possibility of coordination through the amino group. A broad absorption was observed for the complex at 3050 cm^{-1} which is attributed in part to OH and NH stretching in the Asp. This absorption can be compared to a strong absorption in the free Asp at 3000 cm^{-1}.

UV-V spectra were done on the complex in both the aqueous solution and the solid state. As shown in Table 6 and Figure 18, for the solid state spectra, the complex exhibited a broad peak near 345 nm and a shoulder at 225 nm. These bands are attributed to charge transfer between the peroxo groups and the metal.

UV-V spectra in the aqueous solution were done in 0.1 M KCL as shown in Table 7 and over a range of pH's in KCL/KOH/HCL solution with an $\mu=0.1$ as shown in Table 15. In the 0.1 KCL the complex showed a single charge transfer absorption at 330 nm. In the pH dependence study, absorptions in the 270-280 nm range were observed for four pH's in the 0.67-1.55 range. An additional absorption characteristic of V(V) peroxo complexes in acid solution was observed at 450 nm at pH's = 0.67, 1.22, and 1.33 (Figure 18) with $\bar{\varepsilon}$ = 90. Absorptions at 260 nm were observed at pH's = 4.98 and 8.60 while no absorptions were resolved for five pH values in the series. As before, these bands are attributed to charge transfer.

A three cycle cyclic voltamogram was done for the complex

with both forward and reverse scans. The results of this study is shown in Table 16 and Figure 17. This system produced the most complex cyclic voltamogram of the systems that were studied. At least two cathodic peaks appeared for each cycle, both forward and reverse with three peaks appearing for the second and third forward cycles. The anodic peaks were very complex with at least four peaks appearing for each cycle, both forward and reverse, and with five peaks appearing for the second and third forward cycles. No reversible processes are apparent for any of the cycles.

3.3. Stability of Some Mo(VI) and V(V) Peroxo Heteroligand Complexes

The stability of the complexes is determined by periodic titrations for peroxo content with Ce(IV) or $Na_2S_2O_3$. Ce(IV) titrations were used for all of the Mo(VI) complexes and for the V(V)-aspartate complex. $Na_2S_2O_3$ was used for the V(V)-nicotinic acid complex.

The molybdenum peroxo heteroligand complexes are as follows: $[MoO(O_2)_2NAH]*H_2O$, $K[MoO(O_2)_2NA]*H_2O$, and $NH_4[MoO(O_2)_2 NA]*H_2O$. The Mo(VI)- NA complexes are very stable with regard to decrease in peroxo content with decomposition percentages in the range of 0-2% per month.

The Mo(VI)-Asp complex is much less stable with decomposition occurring as much as 15% per month. The vanadium

peroxo heteroligand complexes are $K[VO(O_2)_2NAH]*H_2O$ and

$K_3[VO(O_2)_2]Asp_2]$. The V(V)-NA complex is the least stable of

the complexes studied, decomposing as much as 6-23% per month

and changing from yellow to brownish-yellow on decomposition.

The V(V)-Asp complex decomposes rapidly in a matter of days if

it is dried over drierite and stored in a vial. The complex

changes from yellow to green to brownish-yellow on decompo-

sition and develops a peculiar odor. If the complex is dried

in vacuo at 50°C for four hours immediately after synthesis

and stored over drierite, it is quite stable, decomposing at a

rate of ~0.5% per month. The decomposition data is listed in

Tables 17 and 18 and shown in Figures 23 and 24.

4.0. Experimental

4.1.0. Synthesis of the New Complexes

4.1.1. Nicotinic Acid Systems

4.1.1.1. $[MoO(O_2)_2NAH]*H_2O$

MoO_3(1.44g, 10mmol) is dissolved in H_2O_2 (30%, 10ml,

88mmol) under heating and stirring at ~65°C. The NAH(1.21g,

10mmol) is added gradually by spatula under continued heating

and stirring. Heating and stirring at ~65°C is continued

until a clear solution is obtained with H_2O_2 (30%) being added

as necessary to maintain the volume at ~10ml and to facilitate

the reaction. The pH will be in the 1-3 range. The bright

yellow complex forms on cooling at room temperature and is

filtered, washed in ethanol (first 50%, and finally 95%), and

dried over drierite.

4.1.1.2. K[Mo(O$_2$)$_2$NA]*H$_2$O

KOH (0.84g, 15mmol) is dissolved in H_2O (5ml) along with

MoO_3 (1.44g, 10mmol) under heating and stirring at ~65°C.

When dissolved, H_2O_2 (30%, 44mmol) is added gradually by

dropping pipette. NAH (1.21g, 10mmol) is added gradually by

spatula under continued heating and stirring at ~65°C.

H_2O_2 (30%) is added as necessary to maintain the volume at ~10

ml and to facilitate the reaction. If the solution remains

cloudy after several hours H_2O_2 (10%) is added under heating at

~70°C until the clear solution is obtained (2-3 minutes). The

pH must be in the 2.5-4.0 range in order to obtain the pure

complex. The bright yellow complex forms in cooling at room

temperature and is filtered, washed, and dried as before.

4.1.1.3. $NH_4[MoO(O_2)_2NA]*H_2O$

MoO_3 (2.85g, 20mmol) is dissolved in H_2O_2 (30%, 15ml, 132mmol) under heating and stirring at ~60°C. NAH (2.45g, 20mmol) is dissolved in H_2O (10ml) and NH_4OH (30%, 2ml, 17mmol). The NAH/NH_4OH solution is boiled until only a weak scent of ammonia remains. The two solutions are mixed together at room temperature. The pH should be in the 2.5-6.0 range. The solution is heated at 60-70°C for ten minutes. The complex forms on cooling at room temperature and is filtered, washed, and dried as before.

4.1.1.4. $K[VO(O_2)_2NAH]*H_2O$

KOH (1.12g, 20mmol) is dissolved in H_2O (10ml) and to this solution V_2O_5 (0.92g, 10mmol V) is added with the solution being heated almost at boiling until everything dissolves. H_2O_2 (30%, 0.5ml, 4.4mmol) is added and the solution becomes yellow. The solution is cooled on ice and H_2O_2 (30%, 5ml, 44mmol) is added under continued cooling. NA (1.2g, 10mmol) is added gradually by spatula under stirring and cooling on ice. The pH is ~4. Stirring on ice is continued until the

clear solution is obtained. The yellow complex forms on
cooling at room temperature and is filtered, washed, and dried
as before.

4.1.2. Aspartic Acid Systems

4.1.2.1. $K_x[MoO(O_2)_yAsp_z]*H_2O$

KOH (0.94g, 17mmol) is dissolved in H_2O (5ml) along with

MoO_3 (1.44g, 10mmol) under heating and stirring at ~50°C.

H_2O_2 (30%, 10ml, 88mmol) is added gradually at room tempera-
ture. Aspartic acid (1.33g, 10mmol) is added gradually by
spatula under heating and stirring at ~50°C. The pH is ~5.
Heating and stirring at ~50°C is continued until the clear
solution is obtained. The yellow complex forms on cooling at
room temperature and is filtered, washed, and dried as before.
Coprecipitation of potassium oxoperoxomolybdates occurs and
renders isolation of the pure complex impossible. In addition
to this it should be noted that this procedure sometimes
produces a polymeric mass.

4.1.2.2. $K_3[VO(O_2)_2Asp_2]$

KOH (1.12g, 20mmol) is dissolved in H_2O (10ml) along with

V_2O_5 (0.91g, 10mmol V) with the solution being heated almost at

boiling until everything dissolves. H_2O_2 (30%, 0.5ml, 4.4mmol)

is added. The solution is yellow. The solution is cooled on

ice and H_2O_2 (30%, 5ml, 44mmol) is added. Aspartic acid (1.2g,

9mmol) is added under stirring and cooling on ice. The pH is

~5. Stirring and cooling on ice is continued for 1.5 hours.

The yellow complex forms within five minutes at room

temperature and is filtered and washed as before. It is

necessary to dry the compound in vacuo at 50°C for 4 hours to

prevent rapid decomposition. The complex is stored over

drierite.

4.2. Physical Measurements of the Complexes

4.2.1. Infrared Spectra

Infrared spectra of the complexes were recorded in nujol

and hexachlorobutadiene mulls. Perkin Elmer spectrophotometer

models #983 and #1320 were used, using the following proce-

dure. A small sample of the complex is finely ground with

mortar and pestle and mulled with 1 or 2 drops of nujol or

hexachlorobutadiene. The mull is spread on either NaCl and

CsBr plates, pressed between the two plates, and inserted into

the IR spectrophotometer sample holder. The sample is scanned

from 4000-600cm for nujol mulls on NaCl plates, from 4000-

200cm for nujol mulls on CsBr plates, and from 4000-1300cm for
hexachorobutadiene mulls on NaCl plates.

4.2.2. UV-V Spectra

UV-V spectra of the complexes were recorded in both the
liquid and solid states on the Beckman Acta VI Spectro-
photometer, using the following procedures. The solid state
spectra were done on nujol mulls of the complexes. A small
sample of the complex is finely ground with mortar and pestle
and mulled with 1 or 2 drops of nujol. The mull is spread on
a polyethylene plate and placed in the sample holder of the
spectrophotometer. The spectrum is obtained in the 900-200cm
region. The liquid state spectra were done on $1*10^{-4}$ - $1*10^{-5}$
M solutions of the complexes using 1cm quartz cuvettes. The
sample is dissolved in a KOH/KCL/HCL buffer solution (100ml,
u=0.1). The spectra are obtained in the 900-200cm region over
a wide range of pH's.

4.2.3. Cyclic Voltametry

A cyclic voltamogram was recorded for each complex, using
the following procedures. The complex is dissolved in KCL
(20ml, 0.5 M) to make a solution that is ~$1*10^{-3}$ M. The
solution is placed in a vial and secured in the sample holder.
The solution is purged with nitrogen and a 3-cycle cyclic
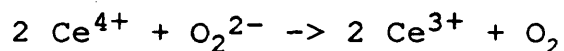
voltamogram is run.

4.3 Analytical Procedures

4.3.1 Analysis of Peroxide

4.3.1.1. Ce(IV) Titrations

A Ce(IV) titration was done for each complex to determine the percentage of peroxide present, based on the following. The reaction is as follows:

$$2\ Ce^{4+} + O_2{}^{2-} \rightarrow 2\ Ce^{3+} + O_2$$

For a typical experiment, 20-30 mg of the complex is weighed by difference on and analytical balance, dissolved in H_2SO_4 (2N, 8ml), and diluted with deionized water (8ml). The solution is titrated against a Ce(IV) solution of known concentration using a Metrohm 655 Dossimat. The volume of Ce(IV) solution needed for the titration is determined and the percentage of peroxide in the complex is calculated.

4.3.1.2. $Na_2S_2O_3$ Titrations

Each vanadium complex was titrated with 0.05XXX $Na_2S_2O_3$ to determine percentage of peroxide and vanadium. The reactions are as follows:

$$V(V) + I^- \rightarrow V(IV) + 1/2 I_2$$

$$4 H^+ + O_2^{2-} + 2 I^- \rightarrow 2 H_2O + I_2$$

$$2 S_2O_3^{2-} + I_2 \rightarrow S_4O_6^{2-} + 2 I^-$$

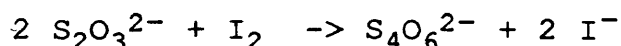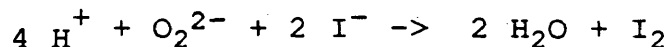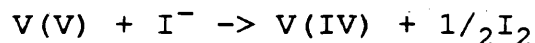The complex is first reduced by excess iodide ion and the iodine produced is reduced by thiosulphate ion. The V(V) to peroxide ratio is 1:2 for monoperoxy species and 1:4 for diperoxy species. For a typical experiment, 20-30 mg of the complex is weighed by difference on an analytical balance and dissolved in deionized water (2-3ml). KI (~0.5g) is added and H_2SO_4 (2N, 10ml) is added. The solution is heated to ~40°C and cooled for 1/2 hour. The cold solution is titrated with 0.05XXX N $Na_2S_2O_3$ solution using starch as an indicator.

4.3.2. Carbon, Hydrogen, and Nitrogen Analysis

C, H, and N analysis of the complexes was done by microanalysis at Atlanta Microlab., Atlanta, Georgia.

5.0. Conclusions

Six new vanadium and molybdenum oxo-peroxo heteroligand complexes have been prepared and characterized. Complexes of

the form $[MoO(O_2)_2NAH]*H_2O$, $K[VO(O_2)_2NAH]*H_2O$, and

$M^I[MoO(O_2)_2NA]*H_2O$ with $M = K^+$ or NH_4^+ have been prepared with

an NAH heteroligand. Complexes of the form $K_x[Mo(O_2)_yAsp_z]*H_2O$

and $K_3[VO(O_2)_2Asp_2]$ have been prepared with an Asp hetero-

ligand. The formation of these complexes is highly dependent

upon the pH, the concentration of each substituent, and the

temperature of the solution. The fact that three biologically

important species: the metal ion, the peroxo group, and the

bioligand come together to form stable complexes is of great

interest in the ongoing study of the role of essential metals

in the living matter.

UV-V spectra show peroxo to metal charge transfer bands

for each of the six complexes and a pH dependence study has

shown that pH does not affect these transitions. This indi-

cates that peroxo coordination persists in aqueous solutions

over the pH range 1-8.

IR spectra show the presence of a coordinated carboxylato

group in each of the complexes. This indicates that the NAH

coordinates as a zwitterion when its net charge is zero, or in

a deprotonated form at higher pH. In the V(V) complex Asp has

a charge of -1, and further work is needed to obtain a pure

Mo(VI) complex of this type.

Cyclic voltametry shows irreversible reduction of more

than one complex of molybdenum species for all the molybdenum

systems studied. More complex electroprocesses are observed

for the $K[VO(O_2)_2NAH] \cdot H_2O$ system and similarly for the

$K_3[VO(O_2)_2Asp_2]$ system. The V(V) systems differ greatly from

the Mo(VI) systems, showing many more oxidation peaks.

In the future, it would be useful to have the x-ray

crystal structure done for the complexes if appropriate

crystals can be obtained. In lieu of the x-ray structure, NMR

would be useful to further elucidate the structure of these

complexes in the aqueous solutions.

Table 3
Analysis of Nicotinic Acid Complexes

Complex	% found					% calculated				
	C	H	N	V	O_2^{2-}	C	H	N	V	O_2^{2-}
$(MoO(O_2)_2NAH)*H_2O$	22.1	2.15	4.30		19.4	22.7	1.91	4.42		20.2
$K(MoO(O_2)_2NAH)*H_2O$	20.7	1.33	3.75		19.4	20.2	1.70	3.93		18.0
$NH_4(MoO(O_2)_2NA)*H_2O$	21.7	2.43	8.47		18.8	21.5	3.01	8.36		19.1
$K(VO(O_2)_2NAH)*H_2O$	20.4	1.97	3.99	16.3	21.1	23.2	1.30	4.52	16.4	20.6
					20.4*					

* From the thiosulphate titrations

Table 4
Analysis of Aspartic Acid Complexes

Complex	% found					% calculated				
	C	H	N	V	O_2^{2-}	C	H	N	V	O_2^{2-}
$K_3[VO(O_2)_2Asp_2]$	19.45	3.22	5.66	12.32	14.56	18.73	2.34	5.46	9.94	12.49
					15.49*					
$K_x[MoO(O_2)_yAsp_2]*H_2O$	8.47	1.51	1.98		11.38					

* From the thiosulphate titrations

Table 5
Infrared Spectra of Nicotinic Acid Complexes

Compound	spectral regions [cm^{-1}]					
	OH	NH and CH	CO, C=C and CH def.	M = O	(O-O)	M-O
Nicotinic Acid	3420 m	3078 w 2930 w	1708 s 1600 m 1588 w	--	--	387 m
[MoO(O$_2$)$_2$NAH]·H$_2$O	3465 m 3340 m	3072 w 2940 w 2880 w	1728 m 1660 s 1590 w	967 s 948 m	874 s 861 m	327 m
K[MoO(O$_2$)$_2$NA]·H$_2$O	3405 m	3117 w 2965 w 2930 w	1676 s 1604 w 1575 w	969 s 949 s	875 s 858 s	324 m 358 m
NH$_4$[MoO(O$_2$)$_2$NA]·H$_2$O	3450 m	3200 w 3145 w 3120 w 3100 w 3065 w 2825 w	1668 s 1628 w 1592 w 1531 w	975 s 944 s	890 s 872 s	342 w 353 w 383 w
K(VO(O$_2$)$_2$NAH)·H$_2$O	3590 m 3510 m	3110 m 3080 w 3000 w 2930 w 2855 w	1740 s 1625 w 1600 w 1585 w	975 s 944 s	890 s 872 s	342 w 353 w 383 w

Table 6
Solid State UV-V Spectra

Compound	λ [nm]
$[MoO(O_2)_2 NAH \cdot H_2O$	276p, 233s
$K[MoO(O_2)_2 NA] \cdot H_2O$	275p, 233s
$NH_4[MoO(O_2)_2 NA] \cdot H_2O$	277p, 235s
$K_x[MoO(O_2)_y Asp_z] \cdot H_2O$	357p, 230s
$K[VO(O_2)_2 NAH] \cdot H_2O$	360p, 230s
$K_3[VO(O_2)_2 Asp_2]$	345p, 225s
NAH	250p
Asp	--

Table 7
UV-V Spectra in 0.1M KCl

Compound	pH	Molar Concentration	λ [nm] $(\mathcal{E}$ [$M^{-1}cm^{-1}$]
$[MoO(O_2)_2 NAH \cdot H_2O$	3.65	saturated	260,300
$K[MoO(O_2)_2 NA] \cdot H_2O$	3.45	8.0×10^{-5}	258
$K_x[MoO(O_2)_y Asp_z] \cdot H_2O$	3.55	6.0×10^{-5}	257,300
$K_x[MoO(O_2)_y Asp_z] \cdot H_2O$	4.15	saturated	290
$K[VO(O_2)_2 NAH] \cdot H_2O$	4.41	3.0×10^{-4}	265, 333 (286)
$K_3[VO(O_2)_2 Asp_2]$	4.16	1.2×10^{-3}	330
NAH	3.96	1.1×10^{-4}	262 (3500)
Asp	3.32	1.7×10^{-3}	--

Table 8

UV-V pH Dependence of $K[MoO(O_2)_2 NAH] \cdot H_2O$

pH	Molar Concentration	λ [nm] ($\mathcal{E}$ [$M^{-1}cm^{-1}$])
0.68	9.8×10^{-5}	257* (1200)
1.17	9.2×10^{-5}	217, 262* (2900)
2.33	1.7×10^{-4}	213, 255* (530), 303 (106)
2.76	7.3×10^{-5}	213, 259* (2200)
3.05	7.3×10^{-5}	214, 256* (1000), 303
3.81	7.9×10^{-5}	205, 259* (1800), 302
4.52	2.2×10^{-4}	255* (420), 308 (250)
5.90	1.5×10^{-4}	259* (1200), 305 (147)
6.99	1.5×10^{-4}	252* (440), 305
8.66	7.9×10^{-5}	255* (510)

* major peak

$\bar{\mathcal{E}} = 1200*, 170$

Table 9

UV-V pH Dependence of $NH_4[MoO(O_2)_2 NA] \cdot H_2O$

pH	Molar Concentration	λ [nm] ($\mathcal{E}$ [$M^{-1}cm^{-1}$])
0.57	9.2×10^{-5}	259 (2700), 325
1.43	1.3×10^{-4}	260 (4400), 300
2.05	7.9×10^{-5}	262 (4200), 305
3.31	1.2×10^{-4}	259 (4700), 300
3.37	9.0×10^{-5}	259 (4700), 300
5.29	9.8×10^{-5}	259 (3700), 300
5.56	8.8×10^{-5}	257 (3300), 300
6.77	5.7×10^{-5}	260 (2400)
7.72	1.4×10^{-4}	257 (2600

$\bar{\mathcal{E}} = 3600$

Table 10

UV-V pH Dependence of $K[VO(O_2)_2 NAH] \cdot H_2O$

pH	Molar Concentration	$\lambda[nm]\ (\varepsilon[M^{-1}cm^{-1}])$
0.55	7.2×10^{-5}	259 (5000)
1.47	1.7×10^{-4}	259 (4000)
2.02	1.2×10^{-4}	258 (2800)
3.08	8.2×10^{-5}	263 (2400)
4.13	1.3×10^{-4}	258 (3200), 320
5.79	4.8×10^{-5}	262 (2200)
7.08	$9.9. \times 10^{-5}$	262 (2900), 325
7.58	5.5×10^{-5}	262 (2700)
	2.1×10^{-4}	262 (2000), 315 (95)

$$\bar{\varepsilon} = 3000,\ 95$$

Table 11

Cyclic Voltametry*

$NH_4[MoO(O_2)_2NA]\cdot H_2O$

Ecathodic	1f	1r	2f	2r	3f	3r
	-610 -1000 -1260	-580 -1000 -1280	-550 -1000 -1250	-550 -880 -1250	-550 -1000 -1260	-600 -980 -1250
Eanodic	1f	1r	2f	2r	3f	3r
	1770	1500	1770	--	1760	--

$K[MoO(O_2)_2NA]\cdot H_2O$
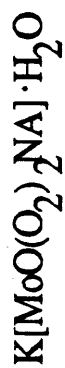
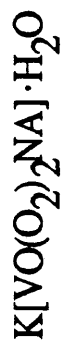| Ecathodic	1f	1r	2f	2r	3f	3r
	-520 -900 -1300	-500 -1800 -1260	-600 -1060 -1300	-600 -720 -1060 -1300	-600 -1060 -1300	-600 -700 -1020 -1270
Eanodic	1f	1r	2f	2r	3f	3r
	1340	1450	1300	1300	1300	1300

* f = forward, r = reverse

Table 12
Cyclic Voltametry*

[MoO(O₂)₂NAH]·H₂O

$[MoO(O_2)_2NAH] \cdot H_2O$

	1f	1r	2f	2r	3f	3r
Ecathodic (mv)	-640 -930 -1210	-530 -630 -810 -1200	-520 -610 -840 -1200	-510 -600 -780 -1200	-520 -610 -800 -1200	-500 -600 -800 -1200
Eanodic (mv)	-240 1440	-200 1360	-230 1500	-260 1430	-260 -1500	-260 1460

K[VO(O₂)₂NA]·H₂O

$K[VO(O_2)_2NA] \cdot H_2O$

	1f	1r	2f	2r	3f	3r
Ecathodic (mv)	-1200	0 -400 -1200	150 -400 -700	130 -300 -740	130 -320 -700	130 -300 -800
Eanodic (mv)	990 1230 140	990 1230 150	990 1220 160	970 1200 100	990 1200 120	970 1190 100

* f = forward, r = reverse

Table 13

Infrared Spectra of Aspartic Acid Complexes

COMPOUND	spectral regions [cm^{-1}]						
	OH	NH	CH	CO	M = O	(O - O)	M - O
Aspartic Acid	3000 s (broad)	3000 s (broad)	3000 s (broad)	1690 m 1650 m 1600 m			
K$_3$[VO(O$_2$)$_2$Asp$_2$]	3050 (s) (broad)	3050 s (broad)	2925 w	1690 m 1650 m 1608 m	973 s 939 s	889 s 870 s	3595
K$_x$[MoO(O$_2$)$_2$Asp$_y$]·H$_2$O	3500 s	3200 s	2920 w 2865 w	1605 s	960 s	900 s 860 m	312 m 360 m

Table 14

UV-V pH Dependence UV-V Study of $K_x[MoO(O_2)_yAsp_z] \cdot H_2O$

pH	Molar Concentration	λ [nm] ($\mathcal{E}$[$M^{-1}cm^{-1}$])
0.66	9.6×10^{-5}	-
1.23	saturated	-
2.06	1.1×10^{-4}	216 (2400)
3.08	6.6×10^{-5}	217 (2300)
4.37	4.5×10^{-5}	203 (2400)
4.97	1.8×10^{-4}	-
6.54	4.2×10^{-5}	204 (2400)
6.90	7.2×10^{-5}	207 (2100)
7.89	saturated	206

$\bar{\mathcal{E}} = 2300$

Table 15

UV-V pH Dependence Study of $K_3[VO(O_2)_2Asp_2]$

pH	Molar Concentration	λ [nm] ($\mathcal{E}$[$M^{-1}cm^{-1}$])
0.67	3.9×10^{-4}	270, 450 (26)
1.22	2.0×10^{-4}	275, 450 (95)
1.33	8.9×10^{-4}	285, 450 (150)
1.55	6.6×10^{-5}	275
2.82	3.0×10^{-4}	-
3.76	1.6×10^{-4}	-
4.74	3.0×10^{-4}	-
4.98	6.9×10^{-5}	260
5.75	3.3×10^{-4}	-
7.10	2.2×10^{-4}	-
8.60	5.2×10^{-5}	260

Table 16
Cyclic Voltametry*

$K_x[MoO(O_2)_y Asp_z] H_2O$

	1f	1r	2f	2r	3f	3r
Ecathodic (mv)	-600 -1000 -1200	-580 -980 -1200	-630 -1000 -1150	-630 -980 -1150	-640 -1000 -1120	-630 -1000 -1140
	1f	1r	2f	2r	3f	3r
Eanodic (mv)	1300	1280	1300	970 1300	1300	870 1300

$K_3[VO(O_2)_2 Asp_2]$

	1f	1r	2f	2r	3f	3r
Ecathodic (mv)	-1780 -2000	-700 -1480	-360 -1160 -2000	-700 -1500	-360 -1160 -2000	-700 -1500
	1f	1r	2f	2r	3f	3r
Eanodic (mv)	-800 260 440 630	-1280 610 980 1180	-1880 -700 20 400 640	-1320 580 980 1160	-1880 -700 50 460 640	-1350 580 1000 1160

*f = forward, r = reverse

Table 17

Decomposition of Some Mo Compounds According to CeIV Titrations

Source Lab Book	Compound	$\%O_2^{2-}$	Date	$\%O_2^{2-}$	%Decomp.	Date
p. 14	[MoO(O$_2$)$_2$NA]·H$_2$O 09/26/84	19.50	10/08/84	15.51	20%	01/17/85
p. 26	[MoO(O$_2$)$_2$NA]·H$_2$O 10/10/84	19.33	10/24/84	19.08	01	11/20/84
p. 12	K[MoO(O$_2$)$_2$NA]·H$_2$O 09/26/84	18.35	10/08/84	12.45	32	11/17/85
p. 13	K[MoO(O$_2$)$_2$NA]·H$_2$O 09/26/84	14.58	10/08/84	14.12	03	01/17/85
p. 25.	K[MoO(O$_2$)$_2$NA]·H$_2$O 10/10/84	18.12	10/24/84	17.80	02	11/20/84
p. 137	K[MoO(O$_2$)$_2$NA]·H$_2$O 11/05/84	19.16	06/11/85	19.17	00	07/29/85
p. 39	NH$_4$[Mo(O$_2$)$_2$NA]·H$_2$O 11/05/84	18.79	11/15/84	17.98	04	01/17/85
p. 40 first	NH$_4$[Mo(O$_2$)$_2$NA]·H$_2$O 11/05/84	18.56	11/15/84	17.09	08	01/17/85
p. 40 second	NH$_4$[Mo(O$_2$)$_2$NA]·H$_2$O 11/05/84	18.16	11/15/84	17.42	08	01/17/85
p. 41	NH$_4$[Mo(O$_2$)$_2$NA]·H$_2$O 11/12/84	19.13	11/15/84	17.57	08	11/17/85
p. 135	NH$_4$[Mo(O$_2$)$_2$NA]·H$_2$O 06/06/85	18.37	06/06/85	18.00	02	07/27/85
p. 170	K$_2$[MoO(O$_2$)$_y$ Asp$_z$]·H$_2$O	10.19	07/04/85	8.81	14	07/29/85

Table 18
Decomposition of Some Vanadium Compounds

COMPOUND	$\%O_2^{2-}$	DATE	$\%O_2^{2-}$	DATE	$\%O_2^{2-}$	DATE
$K[VO(O_2)_2NA]\cdot H_2O$						
7/03/85	20.53	7/08/85	19.62	7/30/85		
6/05/85	21.43	6/11/85	17.94	7/08/85	13.94	7/30/85
6/05/85	19.39	6/11/85	16.06	7/08/85	14.45	7/30/85
$K_3[VO(O_2)_2Asp_2]$						
11/05/85	14.56	11/05/85	14.28	2/26/85		

Figure 4

1. $[MoO(O_2)_2NAH]H_2O$

2.   NAH
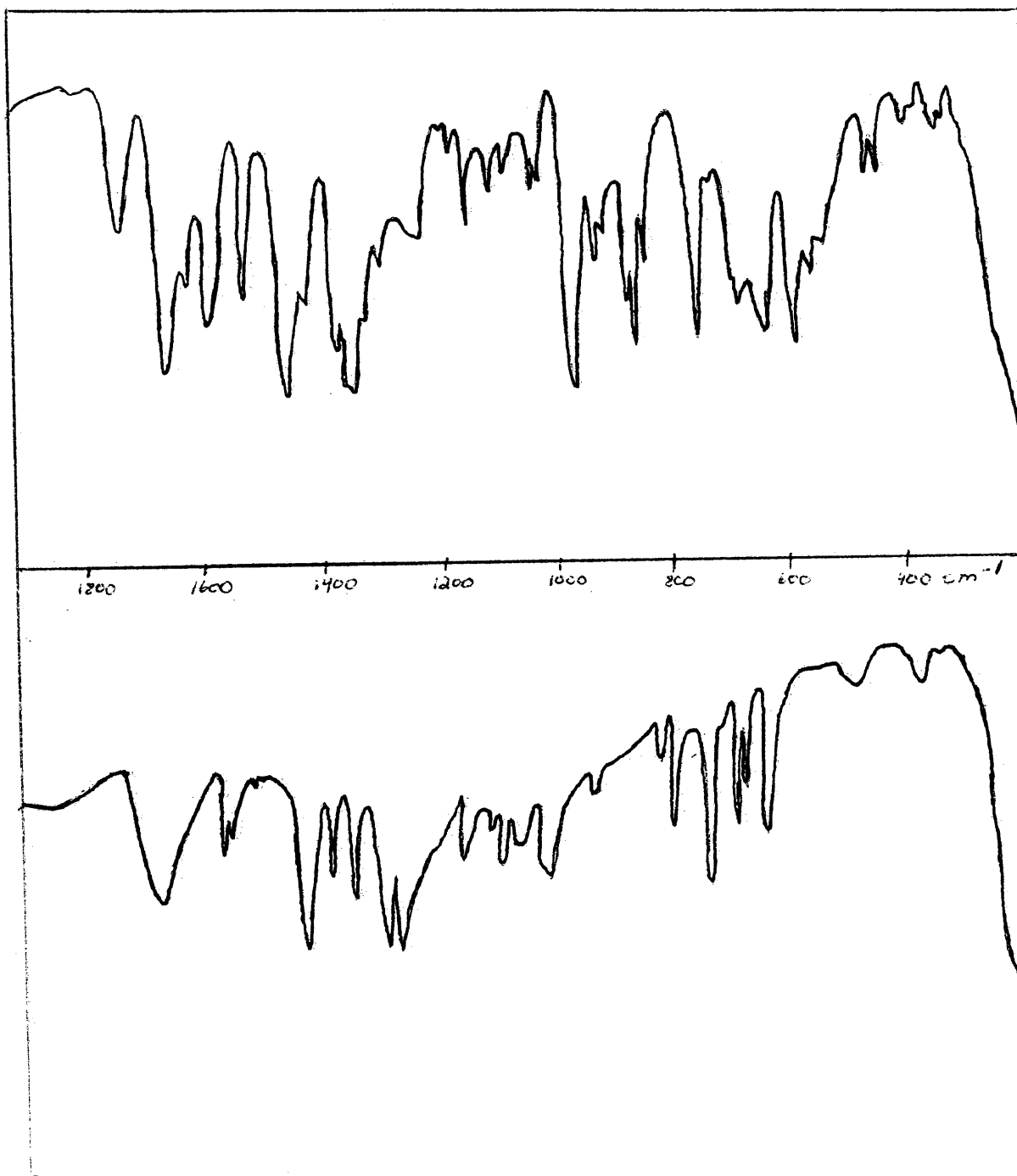
Figure 5

1. $K[MoO(O_2)_2NA]H_2O$
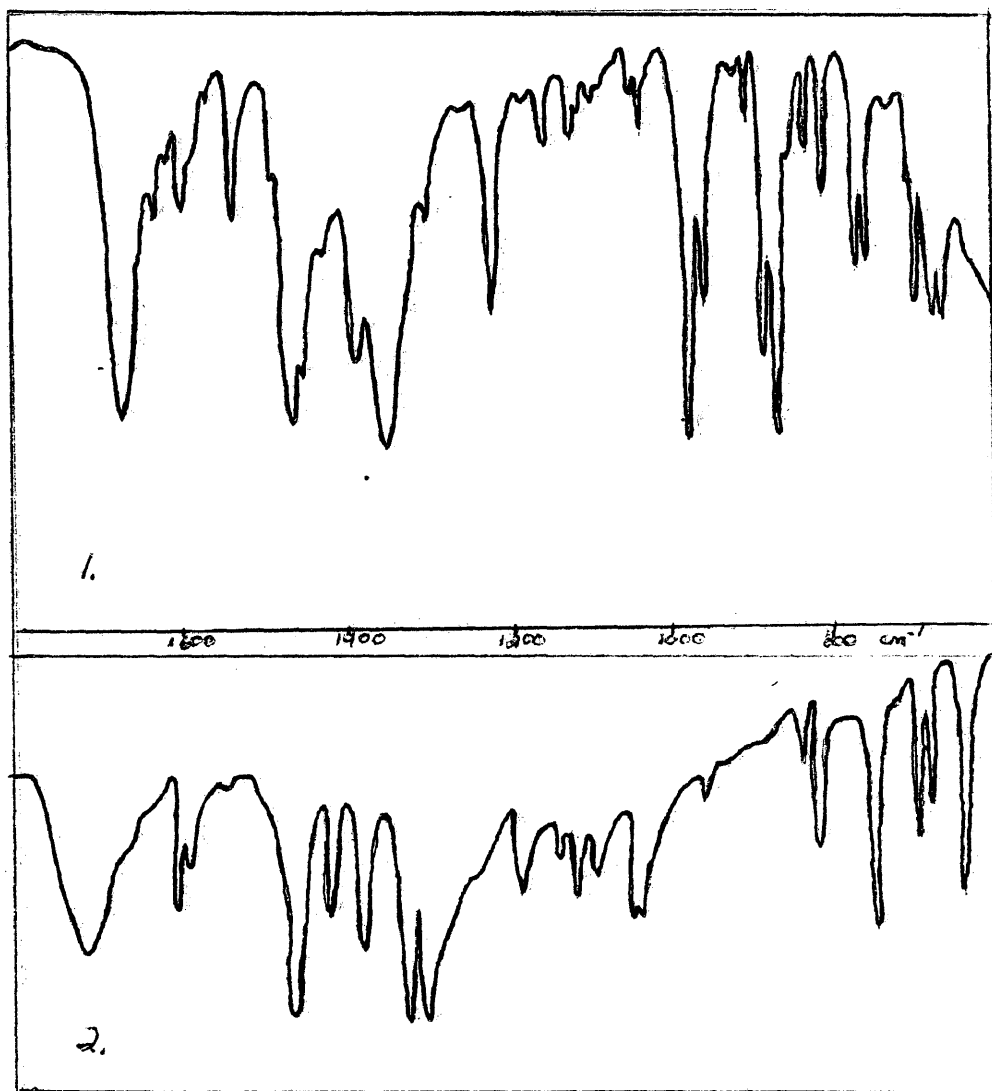
2. NAH

Figure 6

1. $NH_4[MoO(O_2)_2NA]H_2O$

2. NAH
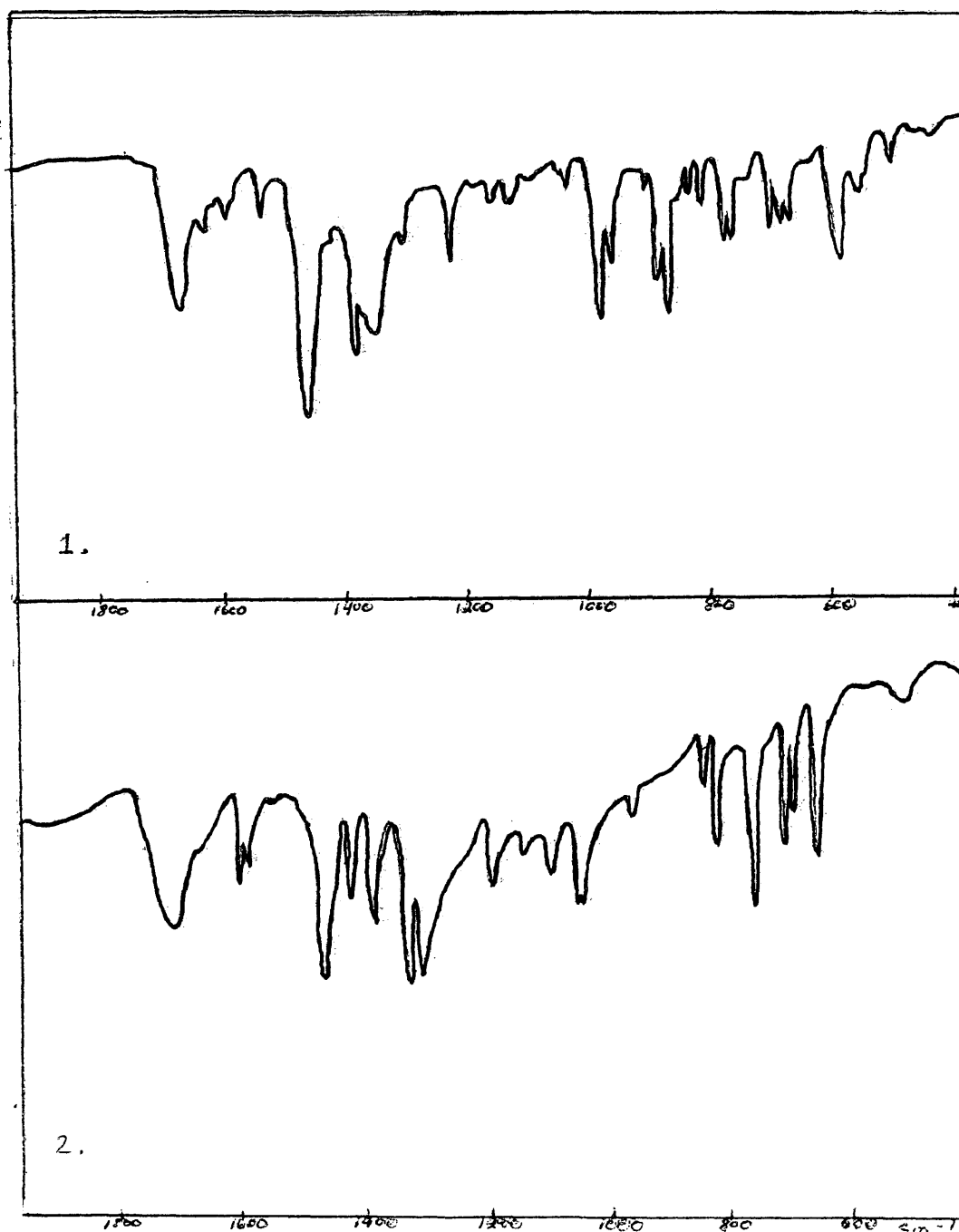
Figure 7

1. $K[VO(O_2)_2NAH]H_2O$

2.   NAH
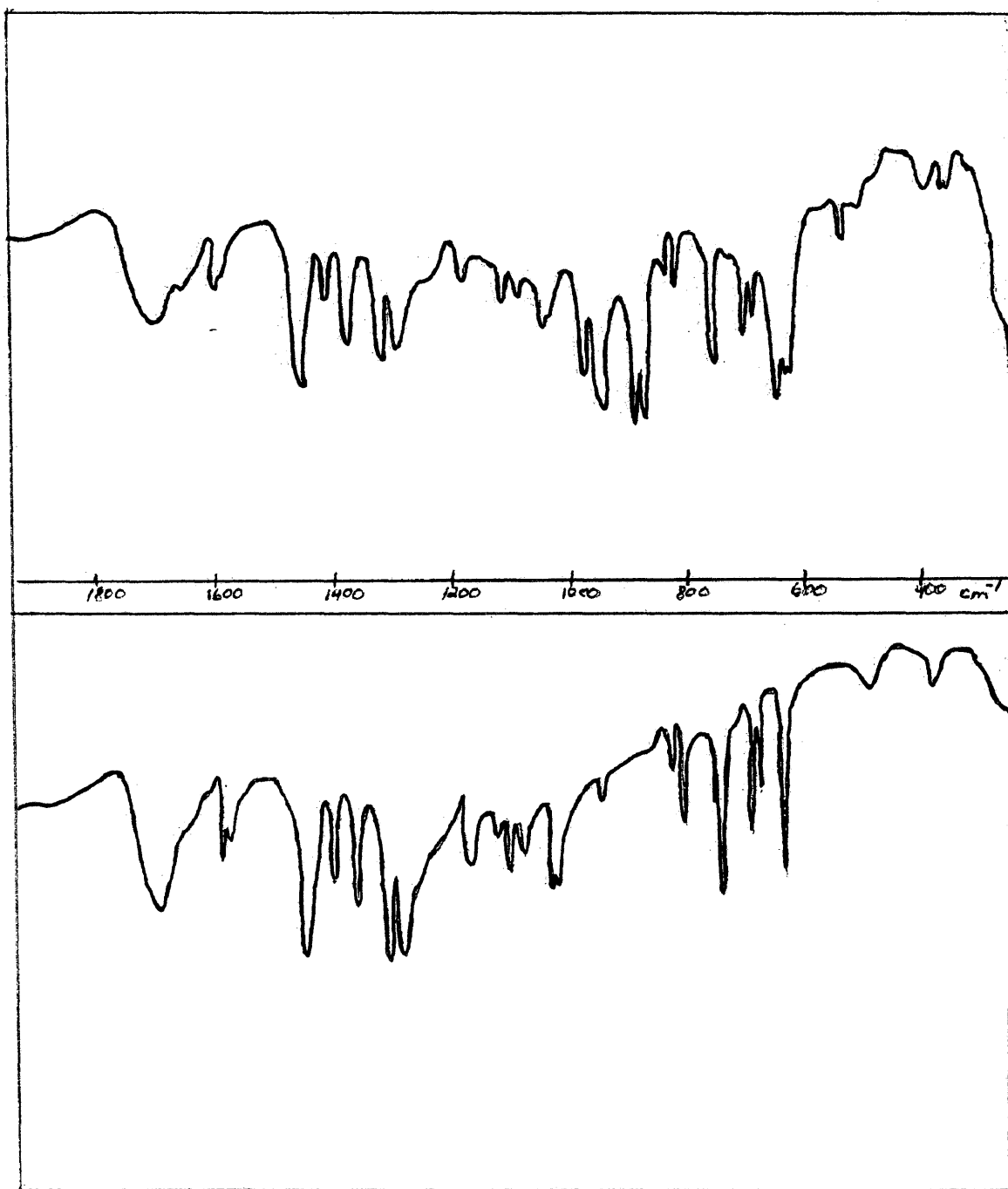
Figure 8

1. $K_x[MoO(O_2)_y Asp_z]$ H_2O

2. Asp
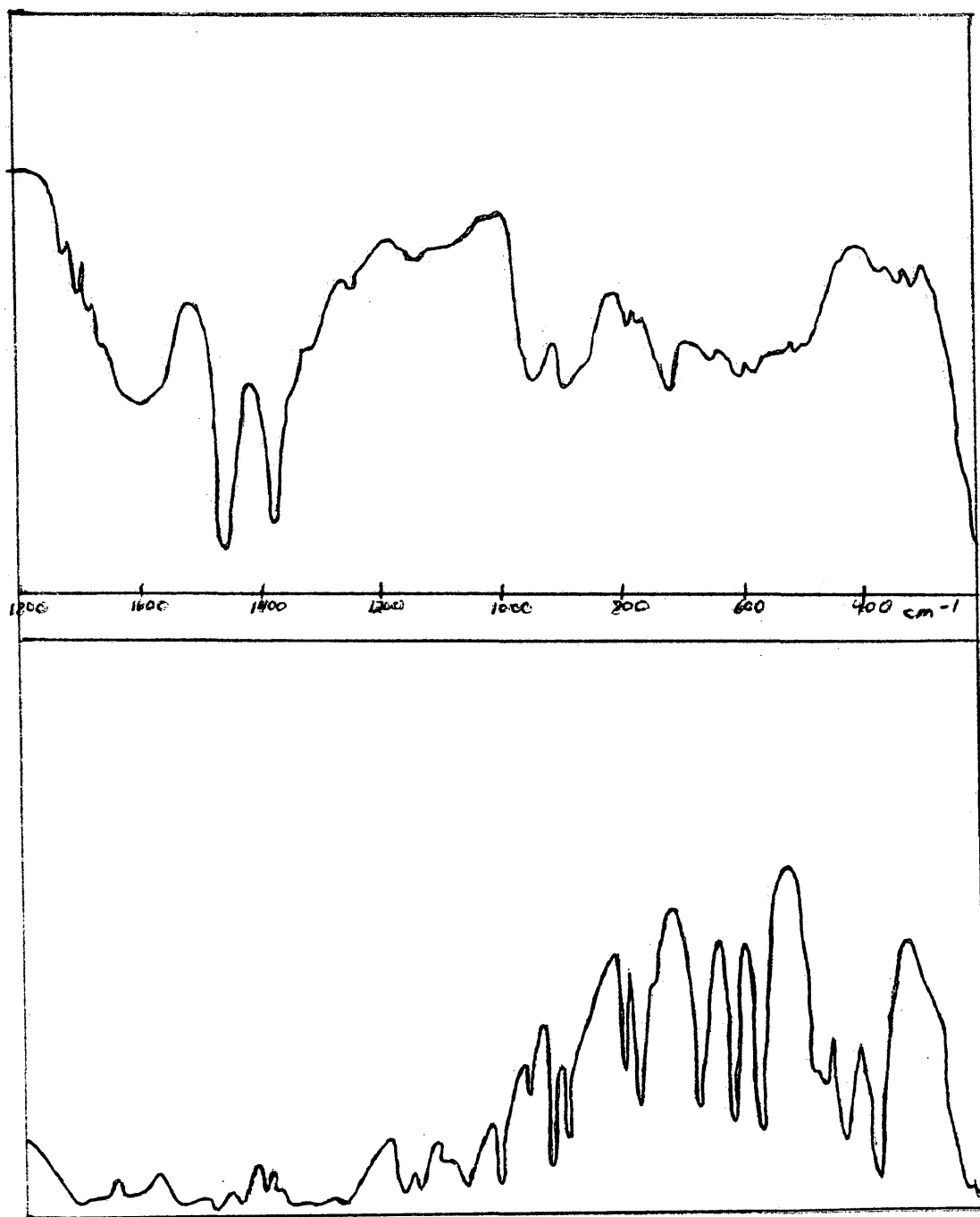
Figure 9

1. $K_3[VO(O_2)_2Asp_2]$

2. Asp
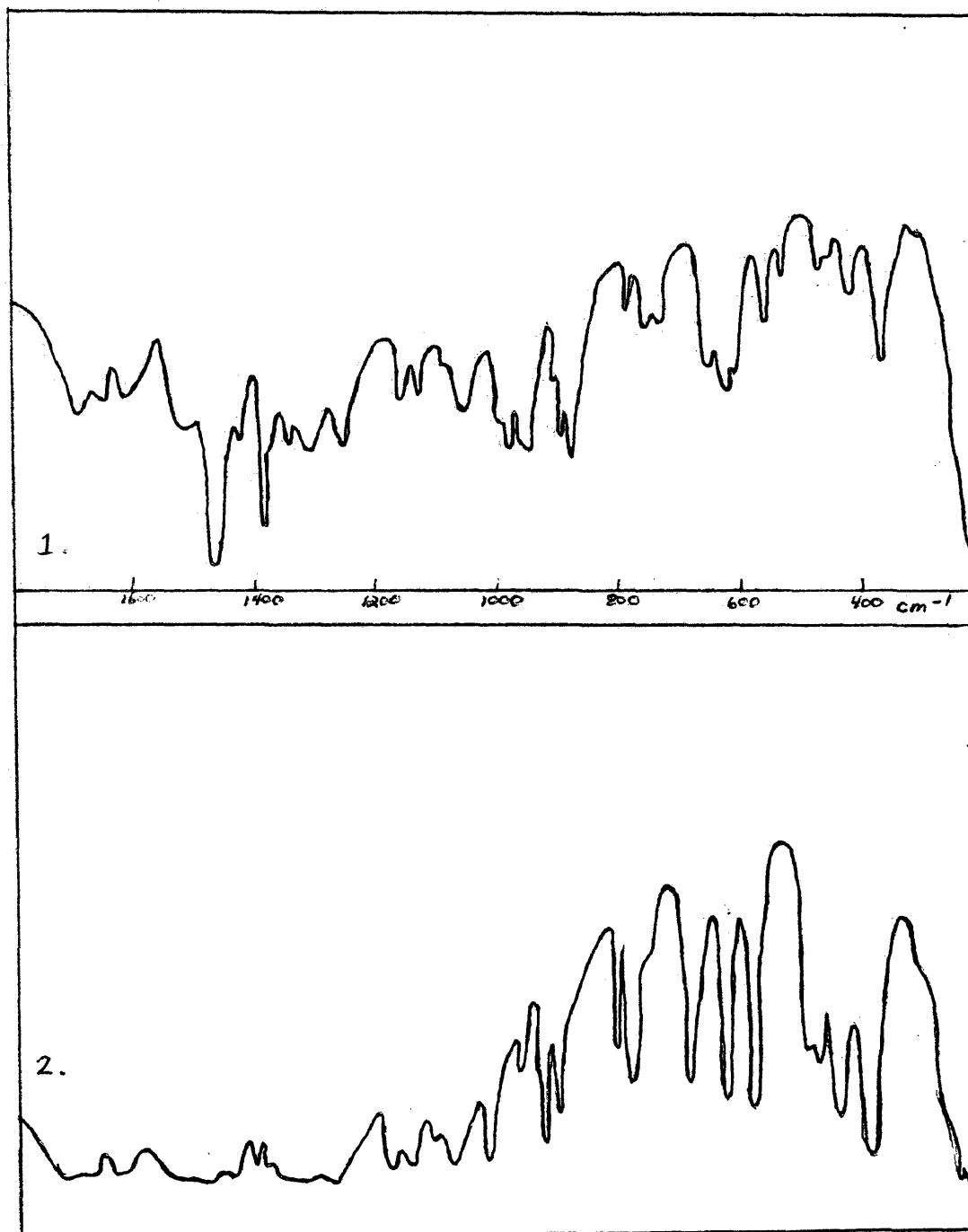
Figure 10

Distorted Pentagonal Bipyramid
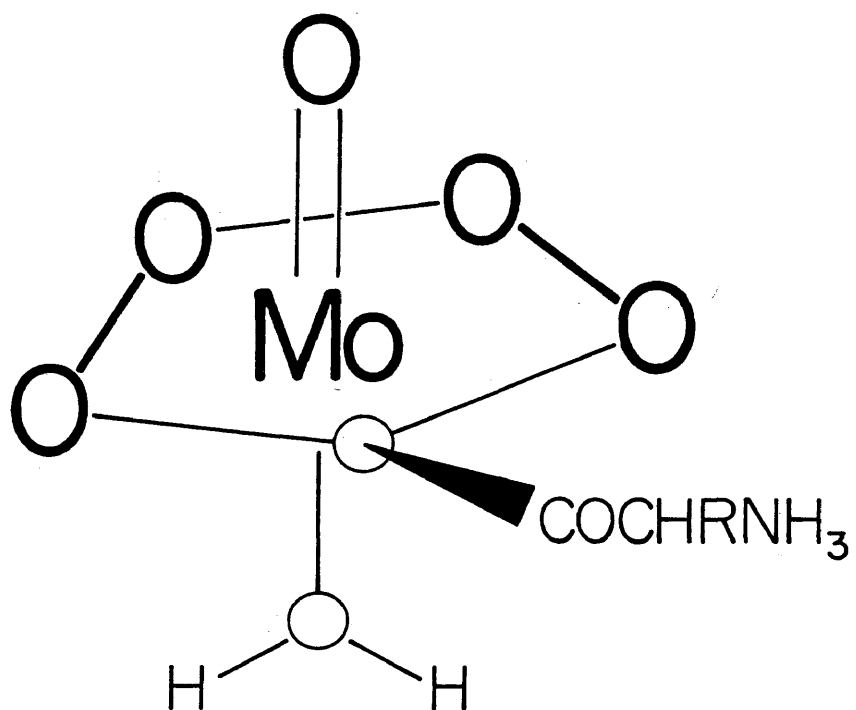
Figure 11

Figure 12

$K[MoO(O_2)_2\, NA]H_2O$

solid state

0.1 M KCl solution

200   300   400   500   600 nm

Figure 13

K[VO(O$_2$)$_2$ NAH]H$_2$O

solid state

O.IM KCl solution

Figure 14

MoO(O$_2$)$_2$NAH

1.00V

K$_x$[MoO(O$_2$)$_y$ASP]

1.00V

K[MoO(O$_2$)$_2$NA]

1.00V

Figure 15

MoO(O$_2$)$_2$NAH

1.00V

NH$_4$[MoO(O$_2$)$_2$NA]

1.00V

K[VO(O$_2$)$_2$NA]

1.00V

Figure 16

$K[VO(O_2)_2NAH]$

1.00 V

1.00 V

Figure 17

$K_3[VO(O_2)_2Asp_2]$

1.00v

1.00v

Figure 18

$K_3[VO(O_2)_2 AsP_a]$

solid state

$pH = 1.3$

200   300   400   500   600nm
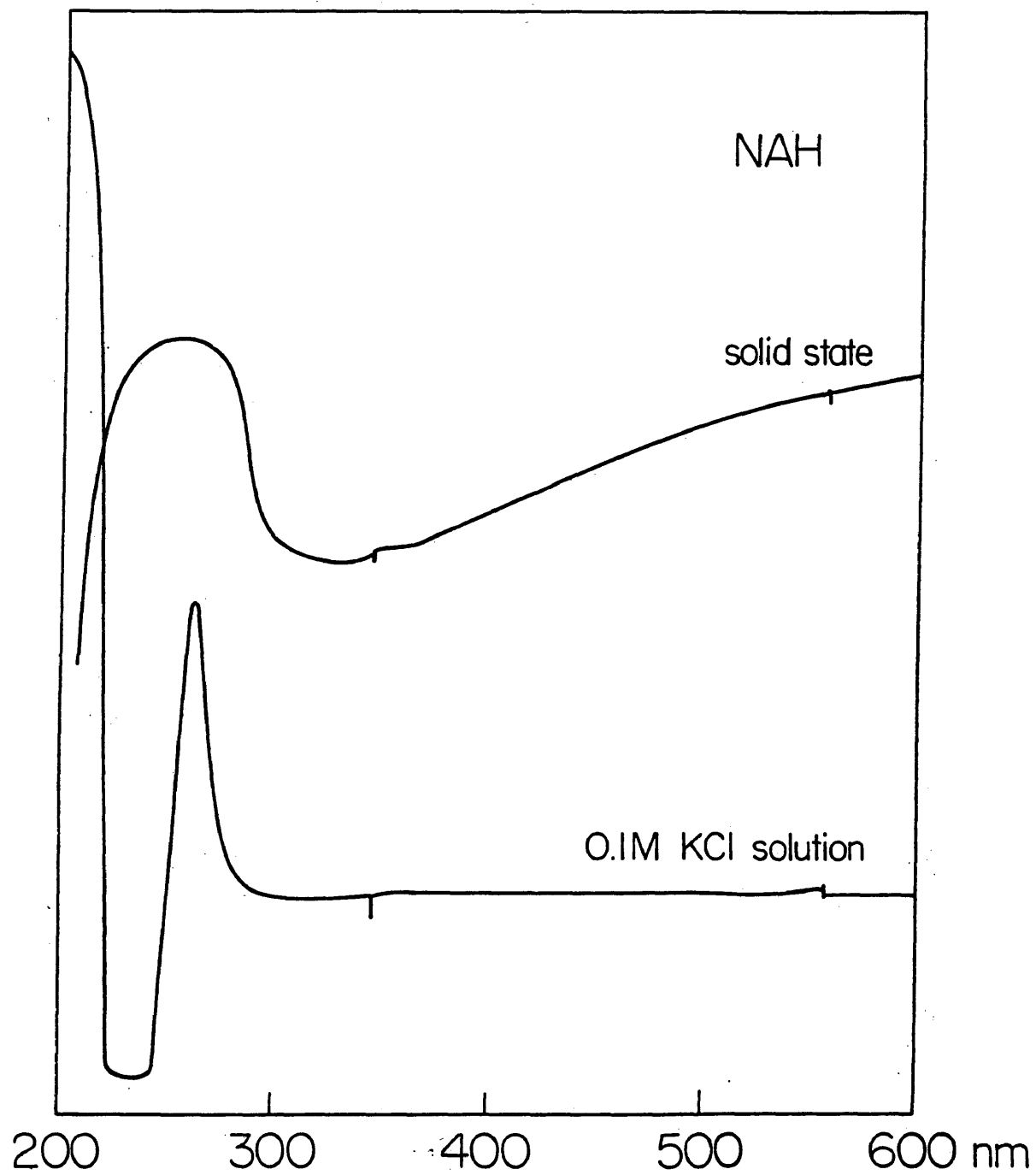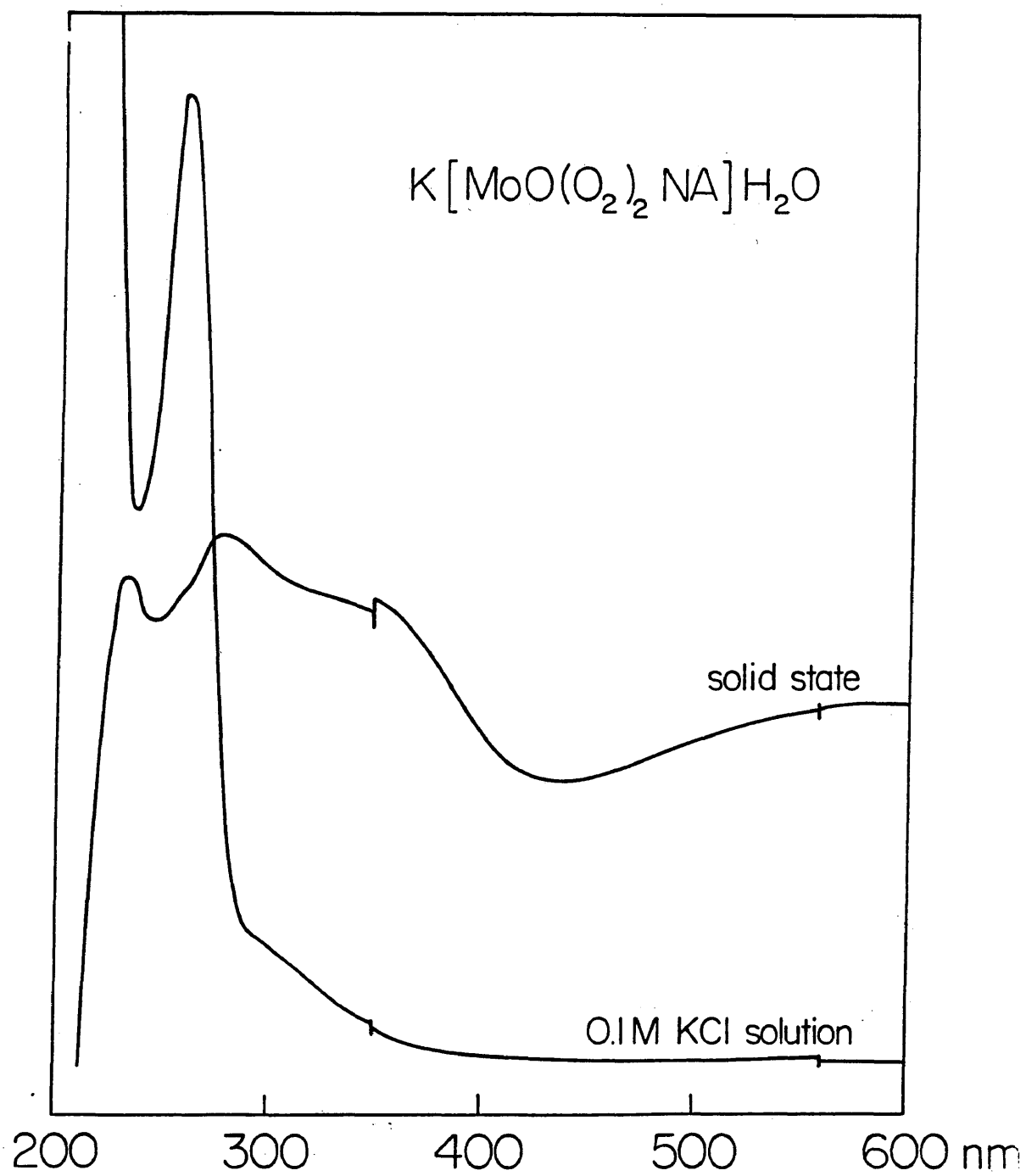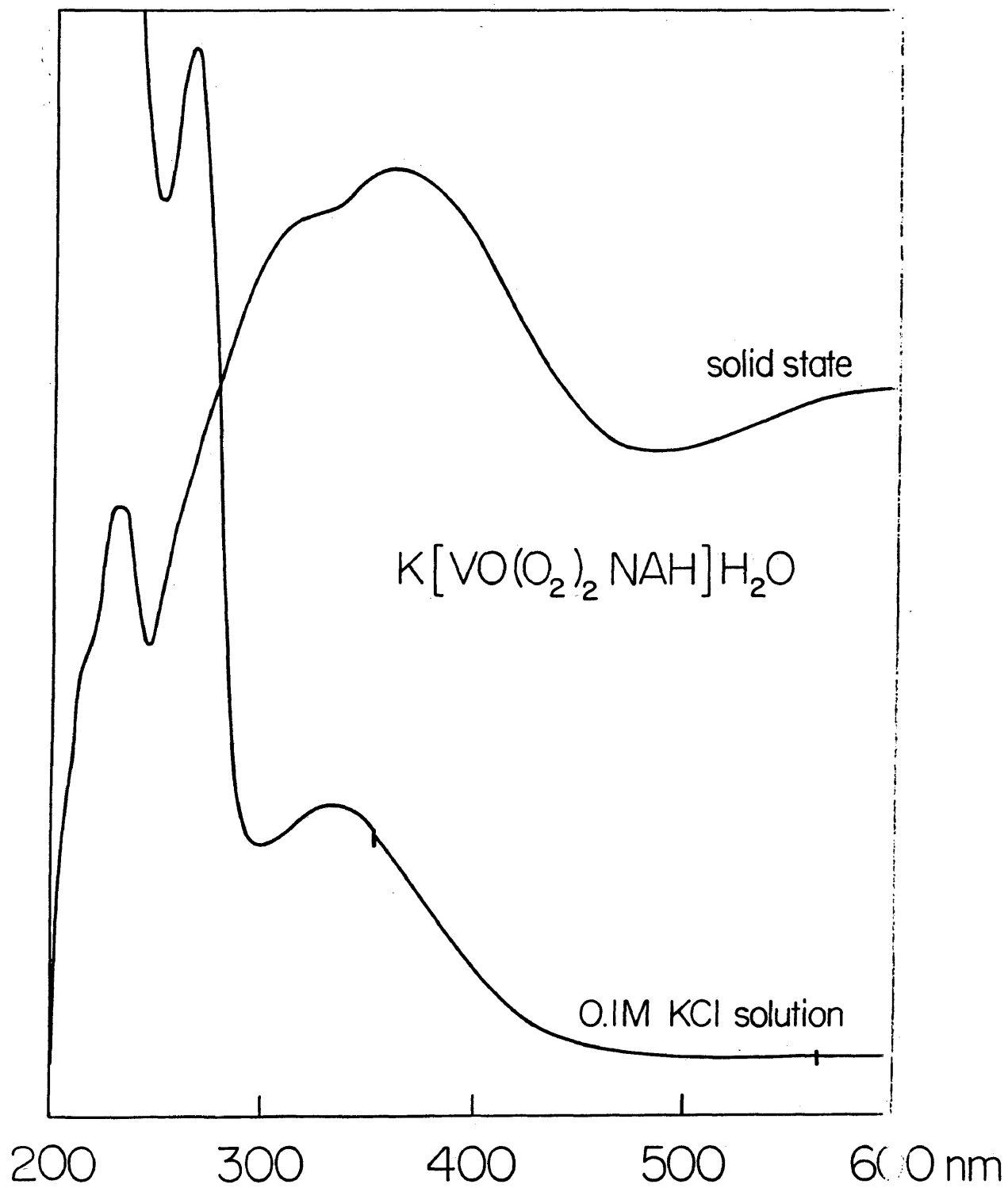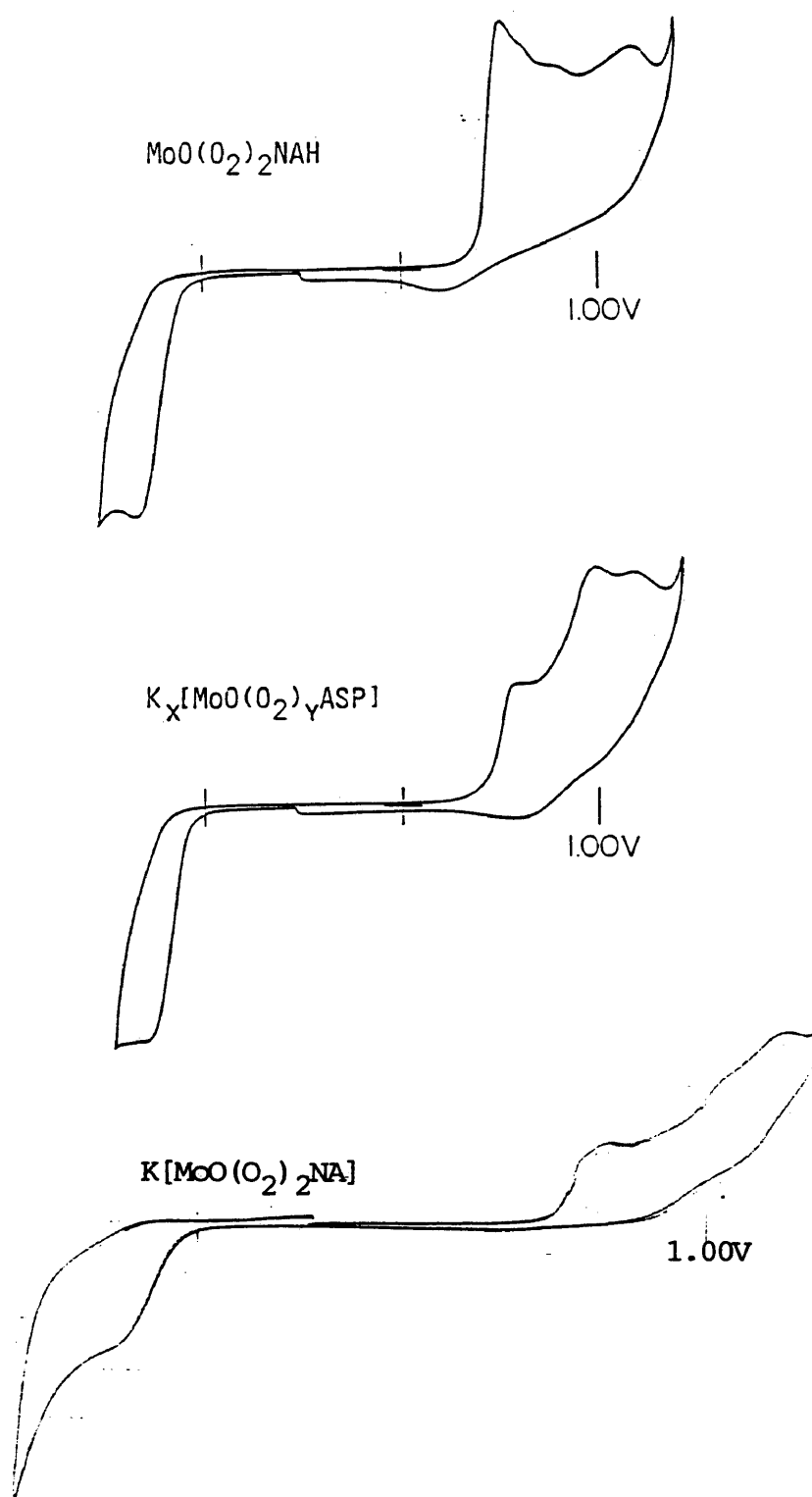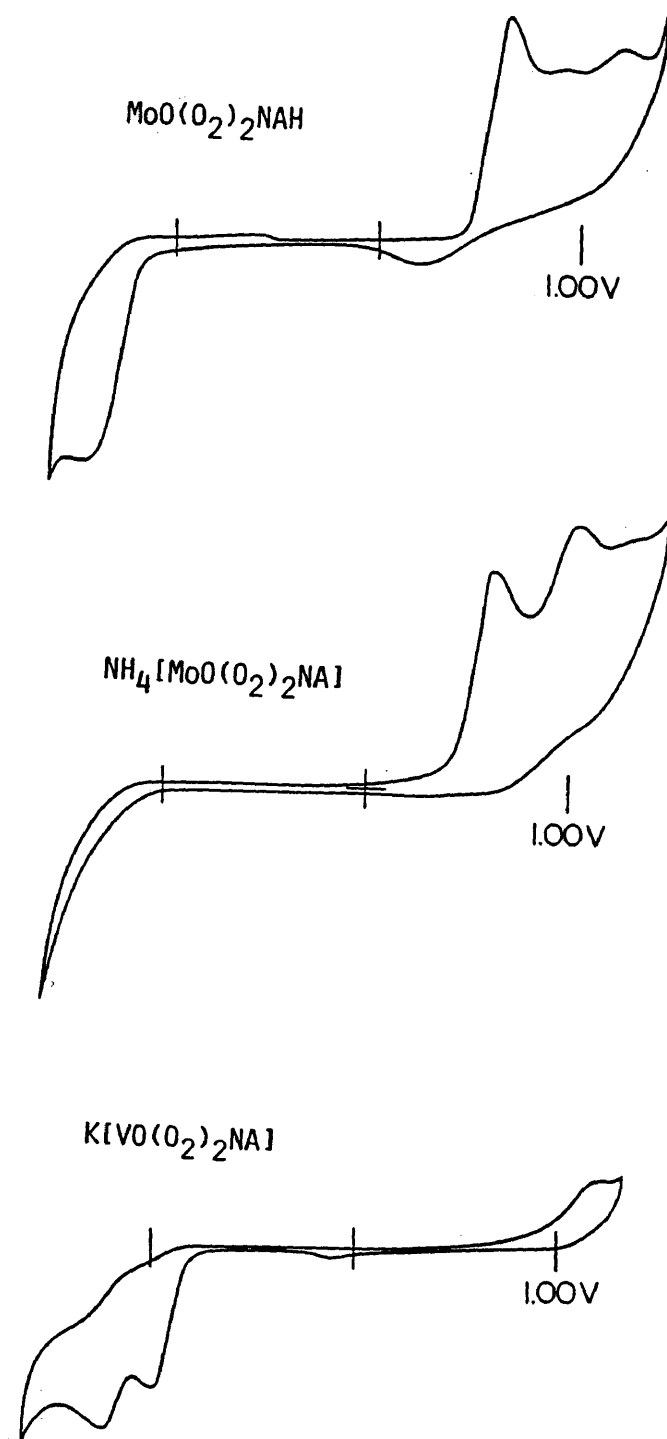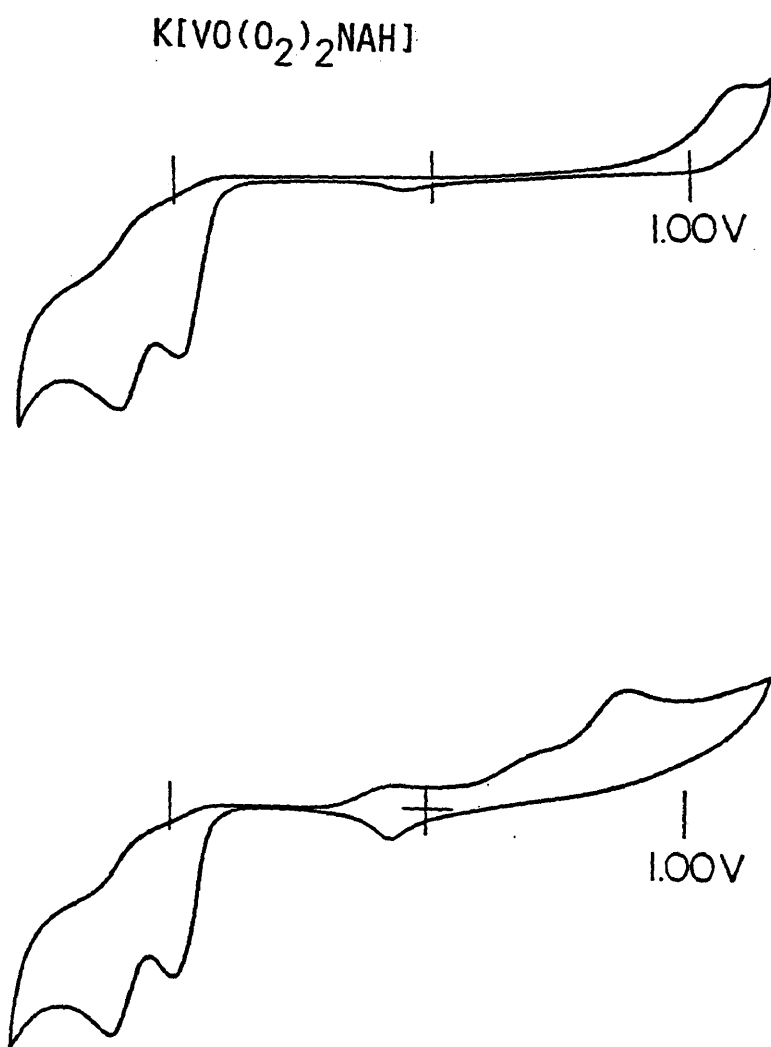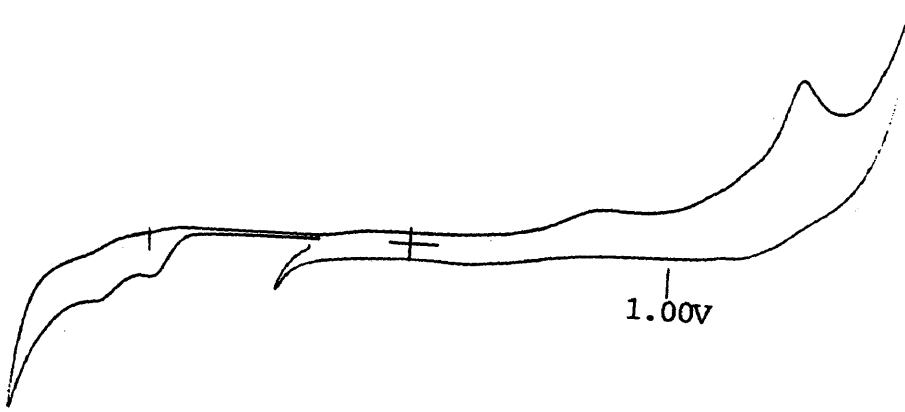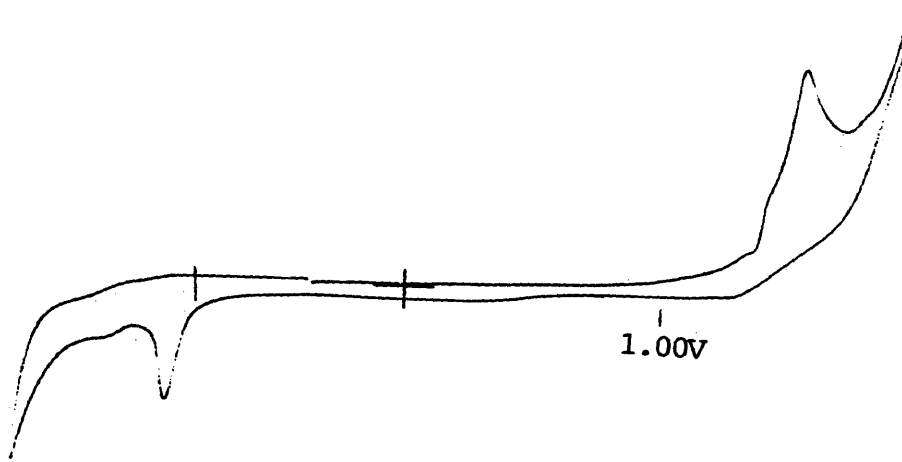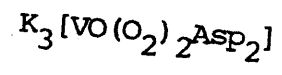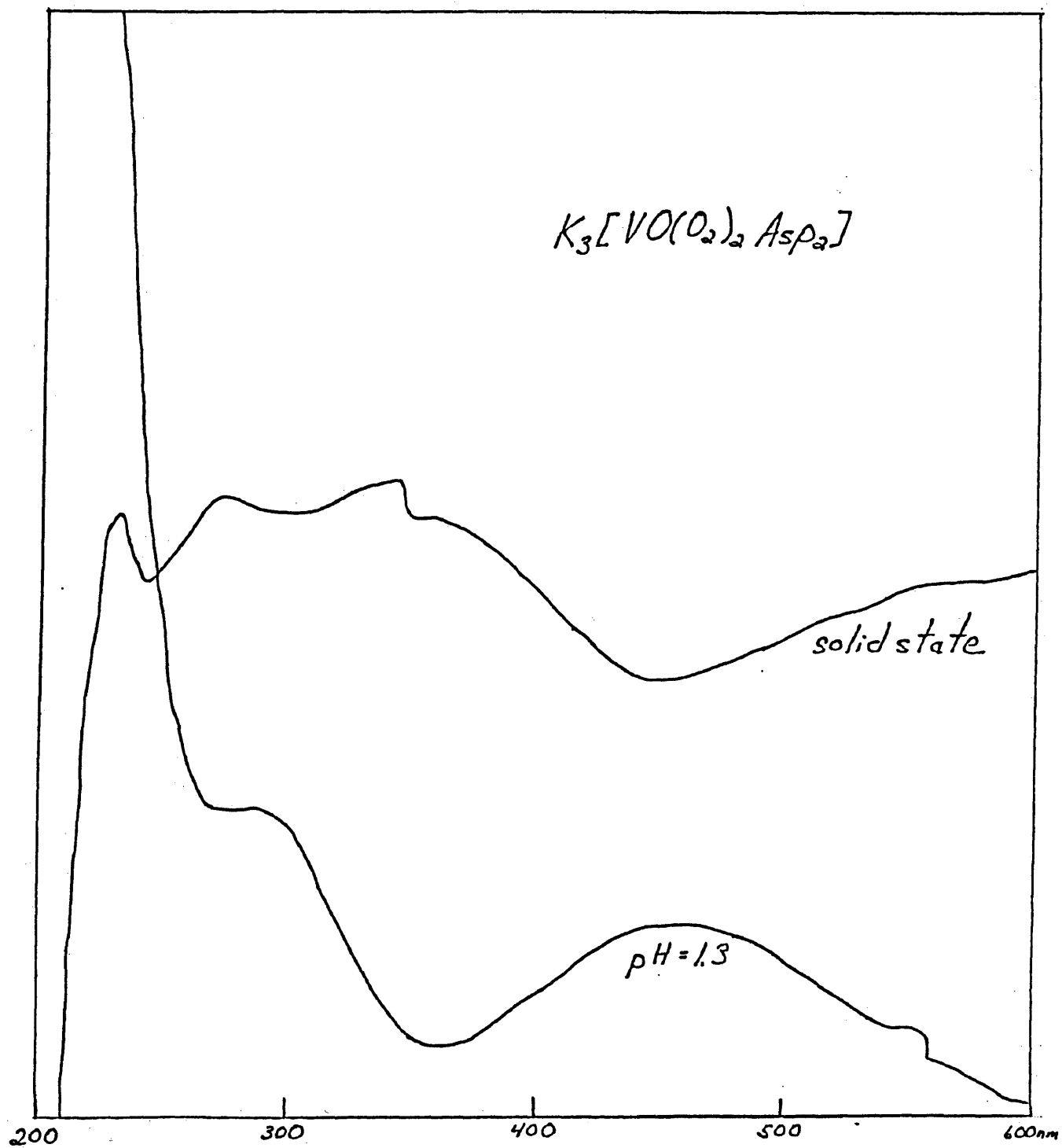
Figure 19

1.   [Mo(O$_2$)$_2$NAH]H$_2$O

2.   NAH
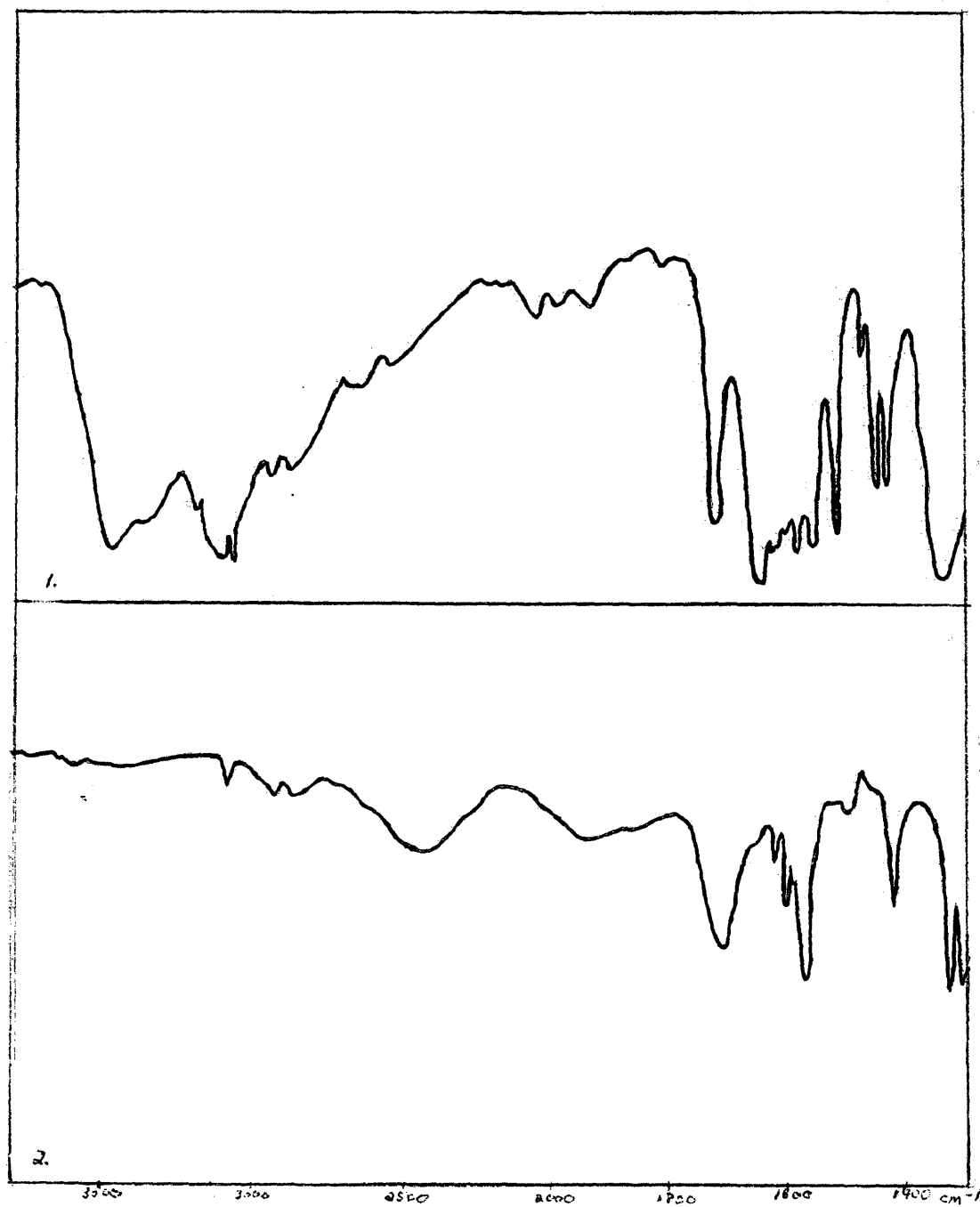
Figure 20

1. $K[Mo(O_2)_2NA]H_2O$

2.   NAH
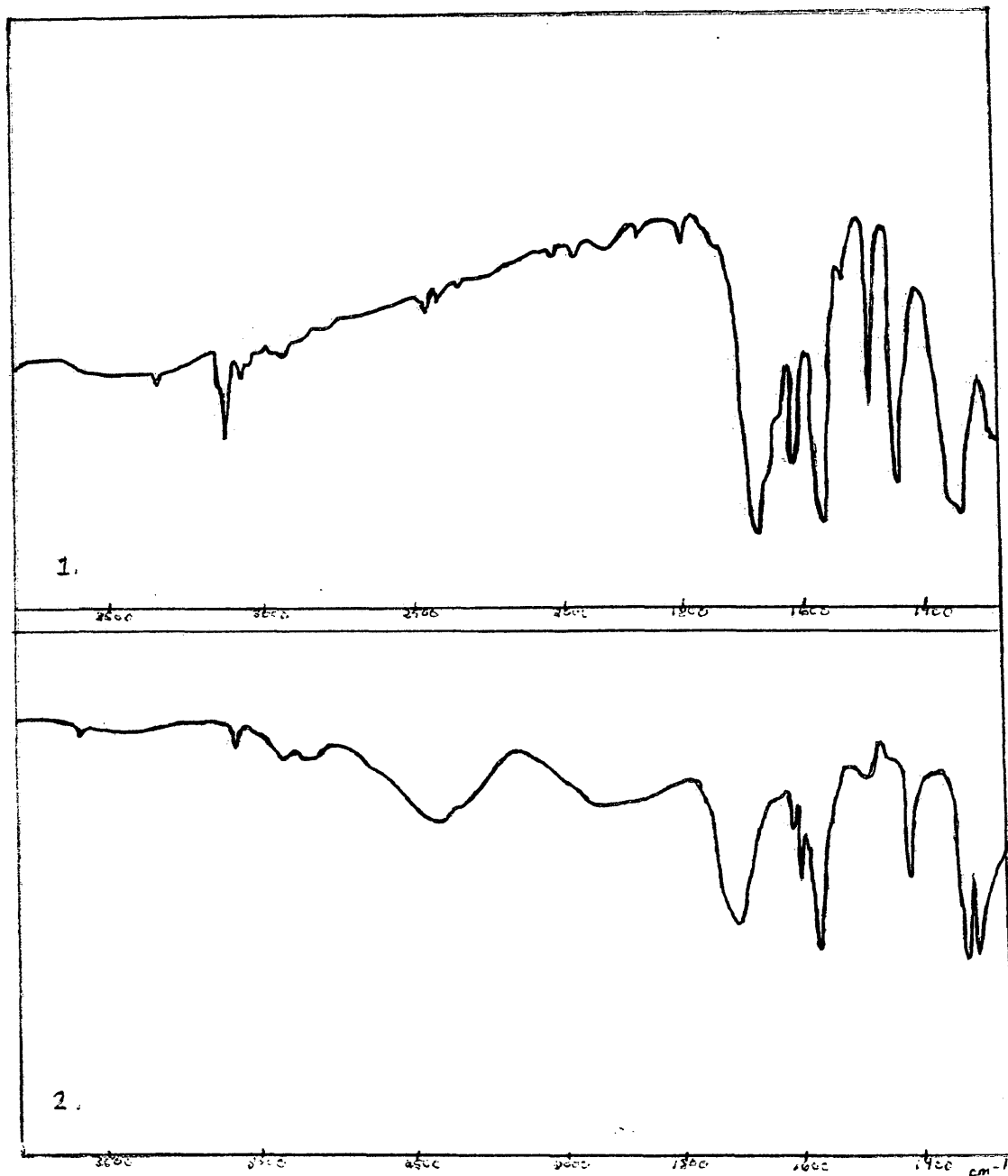
Figure 21

1. $NH_4[Mo(O_2)_2NA]H_2O$

2. NAH
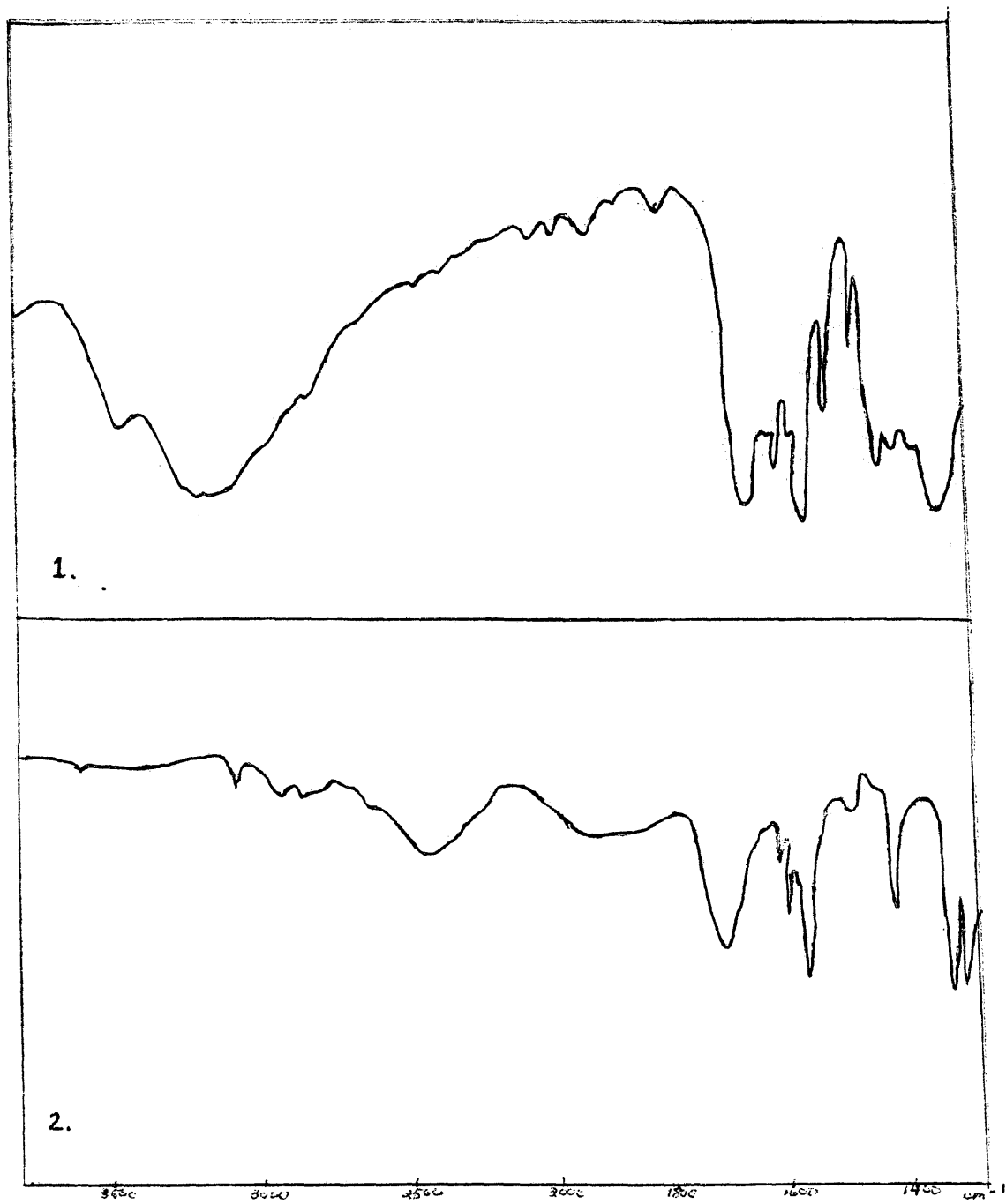
Figure 22

1. $K[VO(O_2)_2NAH]H_2O$

2. NAH
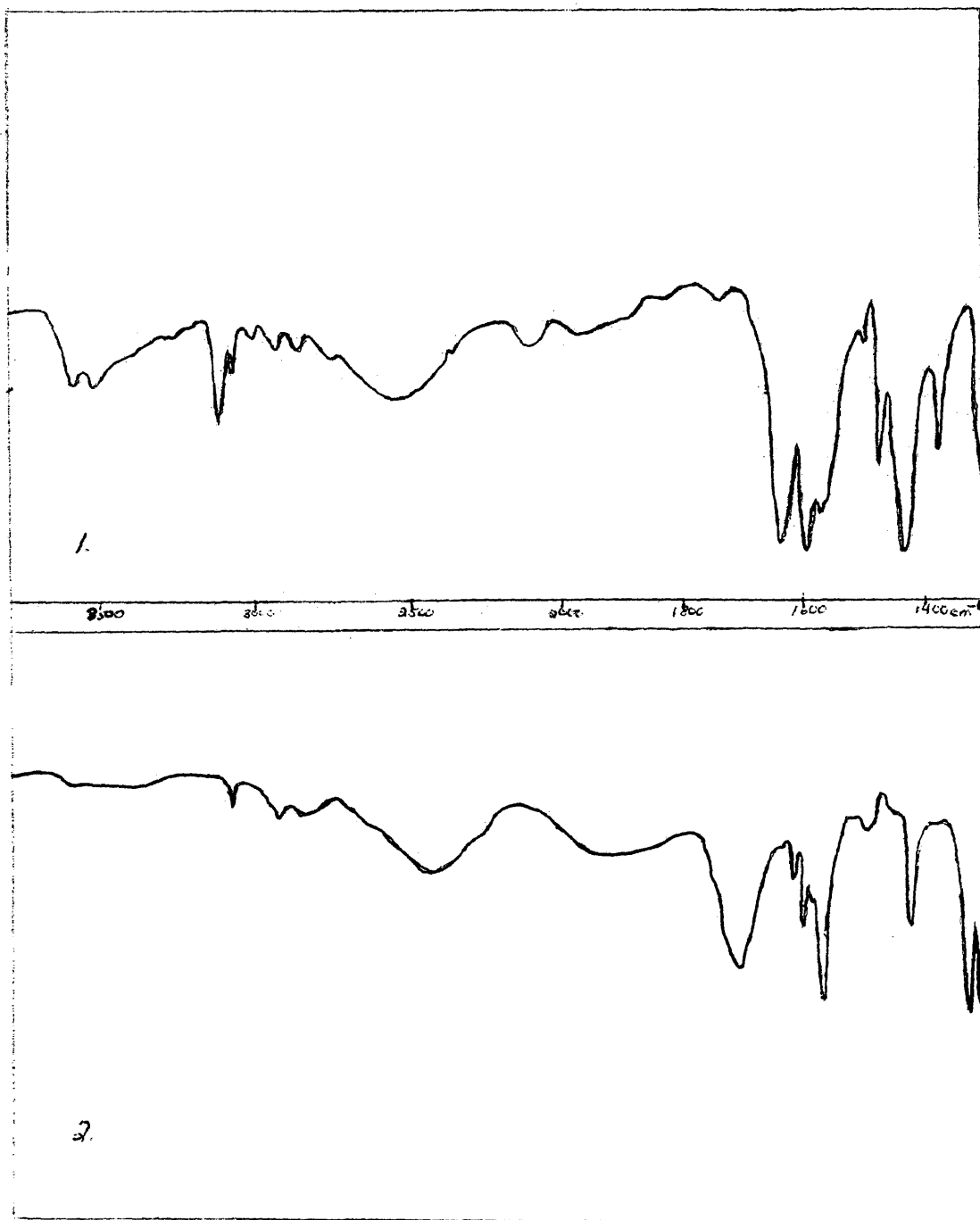
Figure 23

Decomposition Curve

$\circ$ $[Mo\,O(O_2)_2\,NAH]\,H_2O$

$\square$ $K[Mo\,O(O_2)_2\,NA]\,H_2O$

$\triangle$ $NH_4[Mo\,O(O_2)_2\,NA]\,H_2O$

% O_2^{2-}

20

19

18

17

16

15

14

20   40   60   80   100   120   140   160   180

Days

Figure 24

Decomposition Curve

o $K[VO(O_2)_2 NAH]H_2O$

△ $K_3[VO(O_2)_2 Asp_2]$

Days

$\%O_2^{2-}$

83

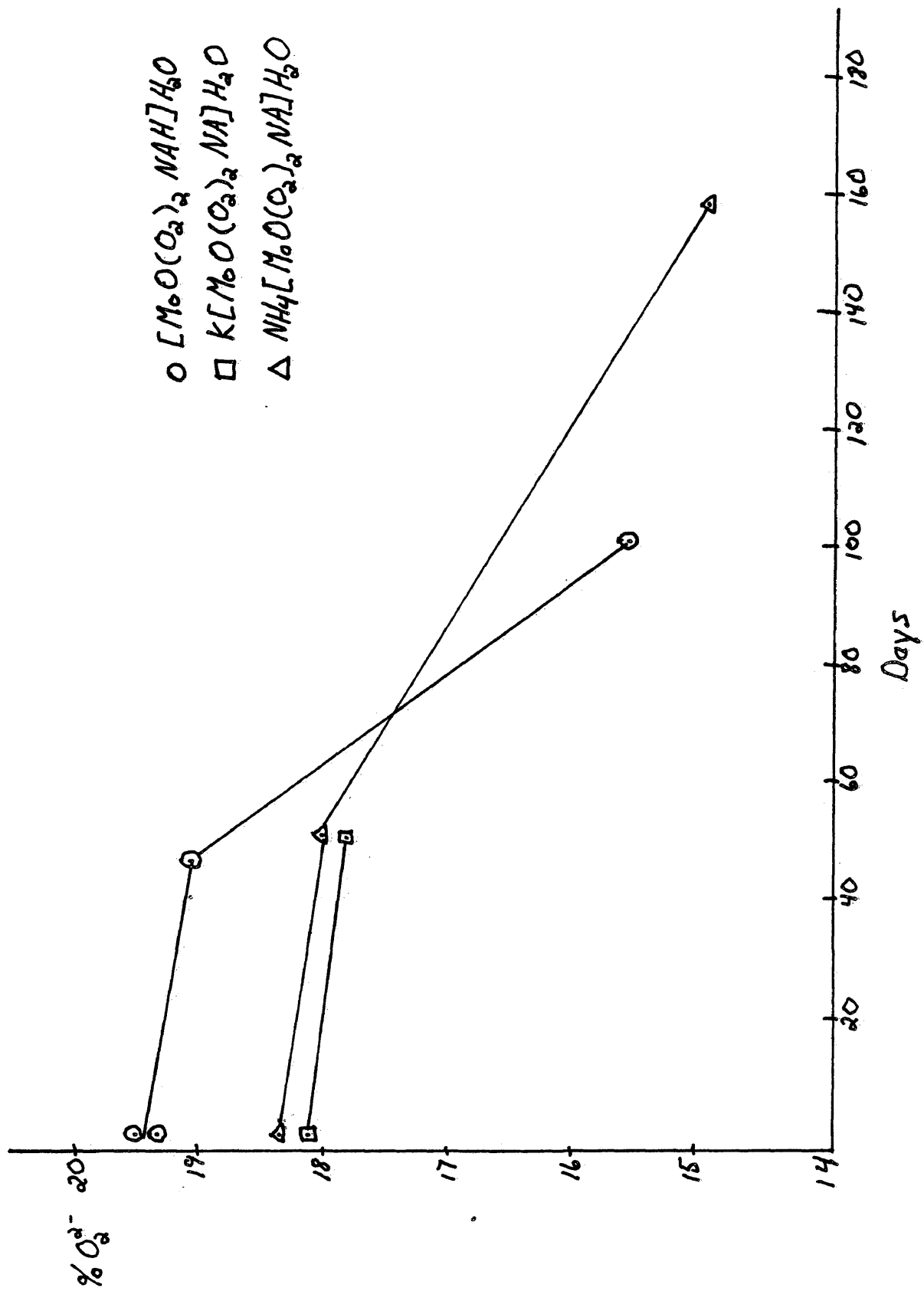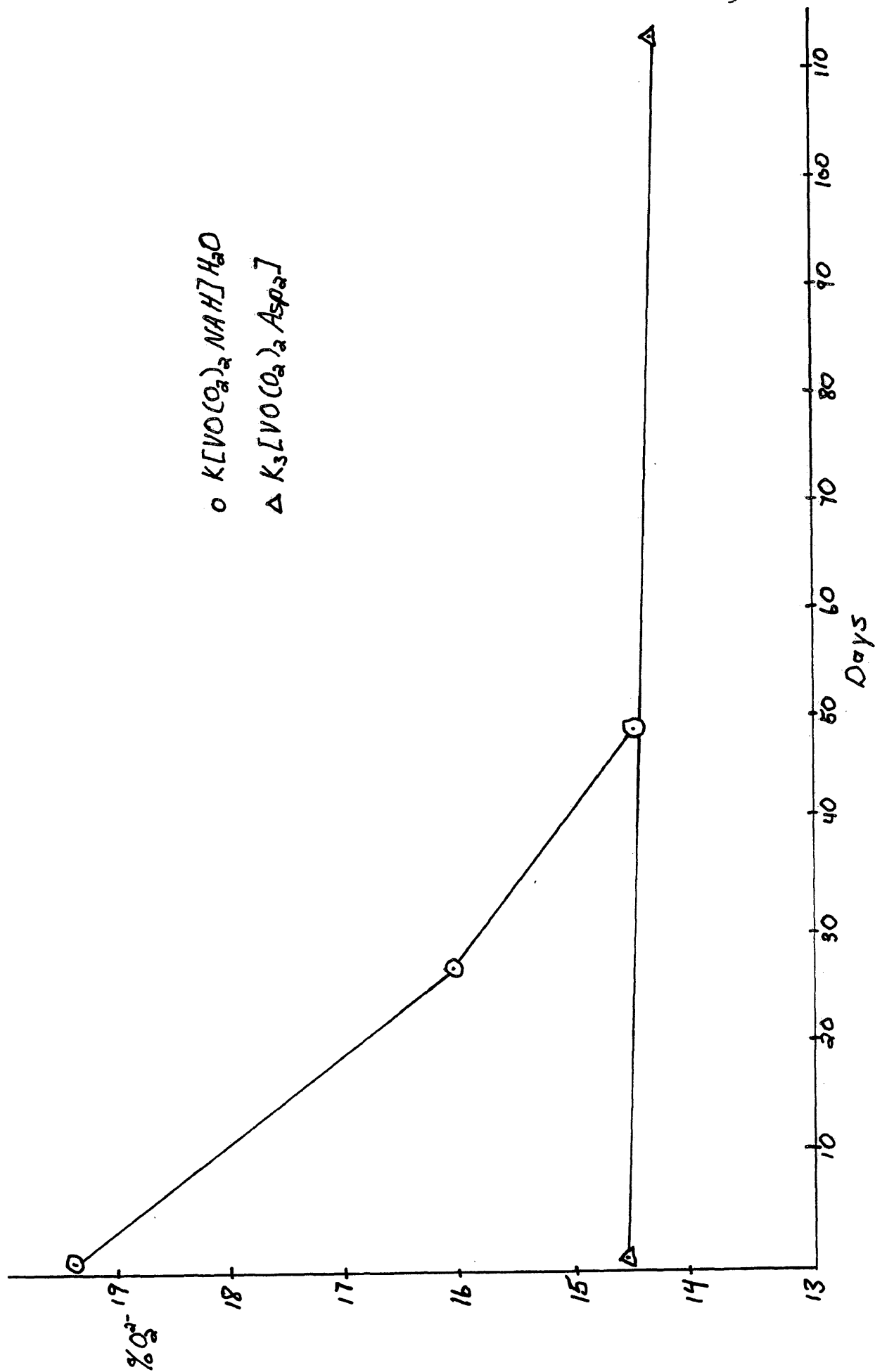## References

1. Cotton, F. A.; Wilkinson, G. "Advanced Inorganic Chemistry";Interscience Publishers: New York, 1972.

2. Emeleus, H. J.; Sharpe, A. G. "Advances in Inorganic Chemistry and Radiochemistry"; Academic Press: New York, 1964.

3. Lippard, S. J. "Progress in Inorganic Chemistry"; 1977, 22, 1.

4. Patai, S. "The Chemistry of Peroxides"; John Wiley and Sons: New York, 1983.

5. Clark, R. J. H.; Brown, D. "The Chemistry of Vanadium, Niobium, and Tantalum"; Pergamon Press: New York, 1973.

6. Eichhorm, G. L. "Inorganic Biochemistry"; Elsevier Scientific Publishing Company: New York, 1973.

7. Sigel, H. "Metal Ions in Biological Systems"; Marcel Dekker, Inc.: New York, 1979.

8. Sundberg, R. J.; Martin, R. B. Chem. Reviews 1974, 74, 471.

9. Speca, A. N.; Gelfand, L. S.; Pytlewski, L. L.; Owens, C.; Karaganiss, N. M. Inorg. Chem. 1976, 15, 1493.

10. Copper, J. A.; Anderson, F.; Buckley, P. D.; Blackwell, L. F. Inorg. Chim. Acta 1984, 15, 1.

11. Broderick, W. E.; Legg, J. I. Inorg. Chem. 1985, 24, 3724.

12. Chang, J. C.; Gerdon, L. E.; Baenziger, N. C.; Goff, H. M. Inorg. Chem. 1983, 22, 1739.

13. Gerdon, L. E.; Goff, H. M. Inorg. Chem. 1982, 21, 3847.

14. Green, C. A.; Biachini, R. J.; Legg, J. I. Inorg. Chem. 1984, 23, 2713.

15. Broderick, W. E.; Legg, J. I. Inorg. Chem. 1985, 24, 3725.

16. Gonzale-Vergara, E.; Hegenauer, J.; Saltman, P.; Sabat, M.; Ibers, J. A. Inorg. Chim. Acta 1982, 66, 115.

17. Gelfand, L. S.; Pytlewski, L. L.; Mikulski, C. M.; Speca, A. N.; Karayannis, N. M. Inorg. Chim. Acta 1979, 33, 265.

18. Knuuttila, H. Acta Chem. Scand. 1983, A37, 765.

19. Knuuttila, H. Inorg. Chim. Acta 1983, 69, 173.

20. Knuuttila, H. Inorg. Chim. Acta 1981, 50, 221.

21. Knuuttila, H. Acta Chem. Scand. 1983, A37, 697.

22. Rabenstein, D. L.; Greenberg, M. S.; Saetre, R. Inorg. Chem. 1977, 16, 1241.

23. Butcher, R. J.; Powell, H. K. J.; Wilkins, C. J.; Yong, S. J. Chem. Soc., Dalton Trans. 1976, 4, 356.

24. Cavaleiro, A. M. V. S. V.; Pedrosa de Jesus, J. D.; Gil, V. M. S.; Gillard, R. D. ; Williams, P. A. Transition Metal Chem. 1982, 7, 75.

25. Antolini, L.; Marcotrigiano, G.; Menabue, L.; Pellacani, G. Inorg. Chem. 1983, 22, 141.

26. Antolini, L.; Marcotrigiano, G.; Menabue, L.; Pellacani, G.; Saladini, M. Inorg. Chem. 1982, 21, 2264.

27. Kirschener, S. J. Am. Chem. Soc. 1956, 78, 2372.

28. Antolini, L; Menabue, L.; Pellacani, G.; Marcotrigiano, G. J. J. Chem. Socl, Dalton Trans. 1982, 7, 2541.

29. Battaglia, L. D.; Corradi, A. B.; Antolini, L.; Marcotrigiano, G.; Menabue, L.; Pellacani, G. C. J. Am. Chem. Soc. 1982, 104, 2407.

30. Watabe, M.; Yano, H.; Odaha, Y.; Kakayashi, H. Inorg. Chem. 1981, 20, 3623.

31. Djordjevic, C.; Vuletic, N.; Sinn, E. Inorg. Chim. Acta 1985, 104, L7.

32. Djordjevic, C.; Covert, K. J. W.; Sinn, E. Inorg. Chim. Acta 1985, 101, L37.

33. Funahashi, S.; Mjdorikawa, T.; Tanaka, M. Inorg. Chem. 1980, 19, 91.

34. Wieghardt, K. Inorg. Chem. 1978, 17, 57.

35. Djordjevic, C.; Vuletic, N. J. Chem. Soc., Dalton Trans. 1973, 93, 1137.

36. Mimoun, H.; Saussine, L.; Daire, E.; Postel, M.; Fischer, J.; Weiss, R. J. Am. Chem. Soc. 1983, 105, 3101.

37. Begin, D.; Einstein, F.; Field, J. Inorg. Chem. 1975, 14, 1785.

38. Drew, R.; Einstein, F. Inorg. Chem. 1973, 12, 829.

39. Djordjevic, C.; Craig, S. Inorg. Chem. 1985, 24, 1281.

VITA

Sandra Jean Sheffield

Born in Petersburg, Virginia, September 19, 1963. Gradu-

ated from Tidewater Academy in Wakefield, Virginia, June 1981,

B.S., College of William and Mary, 1985. M.A. candidate,

College of William and Mary, 1986, with a concentration in

chemistry.